Mechanisms of Development 120 (2003) 919–936

www.elsevier.com/locate/modo

Cloning, expression and relationship of zebrafish *gbx1* and *gbx2* genes to Fgf signaling

Muriel Rhinn[a,1], Klaus Lun[a,1], Angel Amores[b], Yi-Lin Yan[b], John H. Postlethwait[b], Michael Brand[a,*]

[a]*Department of Genetics, Max Planck Institute for Molecular Cell Biology and Genetics, University of Dresden, Pfotenhauer Strasse 108, 01307 Dresden, Germany*

[b]*Institute of Neuroscience, 1254 University of Oregon, Eugene, OR 97403-1254, USA*

Received 12 May 2003; received in revised form 3 June 2003; accepted 5 June 2003

Abstract

The organizer at the midbrain–hindbrain boundary (MHB) forms at the interface between *Otx2* and *Gbx2* expressing cell populations, but how these gene expression domains are set up and integrated with the remaining machinery controlling MHB development is unclear. Here we report the isolation, mapping, chromosomal synteny and spatiotemporal expression of *gbx1* and *gbx2* in zebrafish. We focus in particular on the expression of these genes during development of the midbrain–hindbrain territory. Our results suggest that these genes function in this area in a complex fashion, as evidenced by their highly dynamic expression patterns and relation to Fgf signaling. Analysis of *gbx1* and *gbx2* expression during formation of the MHB in mutant embryos for *pax2.1*, *fgf8* and *pou2* (*noi*, *ace*, *spg*), as well as Fgf-inhibition experiments, show that *gbx1* acts upstream of these genes in MHB development. In contrast, *gbx2* activation requires *ace* (*fgf8*) function, and in the hindbrain primordium, also *spg* (*pou2*). We propose that in zebrafish, *gbx* genes act repeatedly in MHB development, with *gbx1* acting during the positioning period of the MHB at gastrula stages, and *gbx2* functioning after initial formation of the MHB, from late gastrulation stages onwards. Transplantation studies furthermore reveal that at the gastrula stage, Fgf8 signals from the hindbrain primordium into the underlying mesendoderm. Apart from the general involvement of *gbx* genes in MHB development reported also in other vertebrates, these results emphasize that early MHB development can be divided into multiple steps with different genetic requirements with respect to *gbx* gene function and Fgf signaling. Moreover, our results provide an example for switching of a specific gene function of *gbx1* versus *gbx2* between orthologous genes in zebrafish and mammals.

Keywords: *gbx1*; *gbx2*; *otx2*; Midbrain–hindbrain boundary; Isthmus; Organizer; Hindbrain; *Acerebellar*; *No isthmus*; *Spiel-ohne-grenzen*; *fgf8*; *pou2*; Zebrafish

1. Introduction

Generation of cell diversity along the antero-posterior axis in the neuroectoderm is a highly complex process, in which several developmental programs that underlie brain patterning are activated in parallel. Gene expression in the primitive neuroectoderm confers positional information that subdivides the neural plate into differently specified territories, which in turn give rise to the anatomical brain subdivisions. Local organizing centers that arise in the neural plate contribute to this process, and produce signaling molecules that further refine the positional information. One of these organizing centers is established already prior to neural plate stages at the boundary between the mesencephalon and the metencephalon (Martinez et al., 1991; Marin and Puelles, 1994; reviewed by Puelles et al., 1996; Joyner et al., 2000; Rhinn and Brand, 2001; Wurst and Bally-Cuif, 2001). This midbrain–hindbrain boundary (MHB) organizer is later localised at the morphologically visible constriction between the midbrain and hindbrain, called the isthmus rhombencephali, and is thus also known as the isthmic organizer.

The MHB organizer produces secreted signaling molecules that influence patterning in the adjacent tissue along the rostro-caudal axis of the brain. Among the secreted proteins, the vertebrate homologue of the *Drosophila*

* Corresponding author. Tel.: +49-351-210-1350; fax: +49-351-210-1389.

E-mail address: brand@mpi-cbg.de (M. Brand).

[1] These authors contributed equally to this work.

0925-4773/$ - see front matter © 2003 Elsevier Ireland Ltd. All rights reserved.
doi:10.1016/S0925-4773(03)00135-7

wingless gene, *Wnt1* (McMahon et al., 1992) and *Fgf8* play key roles during MHB development and function in mice (Crossley et al., 1996; Meyers et al., 1998) and zebrafish (Reifers et al., 1998; Picker et al., 1999). Ectopic application of FGF8 protein by means of acrylic beads can induce isthmic-like structures in chicken, mice and zebrafish with a gene expression profile characteristic for the MHB (Crossley et al., 1996; Martinez et al., 1999; Liu et al., 1999; M.B., unpublished). Among those genes are several transcription factors that are required during development of the MHB, such as *En1* and *En2* (Wurst et al., 1994; Millen et al., 1994; Scholpp and Brand, 2001), *Pax2*, *Pax5* and *Pax8* (Urbanek et al., 1994; Favor et al., 1996; Brand et al., 1996; Lun and Brand, 1998; Pfeffer et al., 1998), *Otx1* and *Otx2* (Ang et al., 1996; Acampora et al., 1996) and *Gbx2* (Wassarman et al., 1997; Shamim and Mason, 1998; Millet et al., 1999). In order of their appearance, *Otx2* is expressed first (Ang et al., 1994; Li et al., 1994), followed by the onset of *Gbx2* expression in the posterior part of the embryo adjacent to the *Otx2* domain (Wassarman et al., 1997; Martinez-Barbera et al., 2001; Li and Joyner, 2001). *Pax2* is activated at E7-7.5, *En1* and *Wnt1* at E7.75 at the future MHB (Rowitch and McMahon, 1995) and *Fgf8* is activated at E8 in the neuroectoderm (Crossley and Martin, 1995; Shamim et al., 1999). All genes are activated around the *Otx2*/*Gbx2* boundary and this order of expression already suggested that the region where *Otx2* and *Gbx2* abut might demarcate the primordium of the MHB. Recent studies in mouse and chicken showed, that indeed ectopic juxtaposition of *Gbx2* and *Otx2* expression domains can induce MHB marker expression (Hidalgo-Sanchez et al., 1999; Katahira et al., 2000). Misexpression of *Gbx2* in the caudal midbrain represses *Otx2* expression and induces MHB markers (Millet et al., 1999; Tour et al., 2002); similarly, *Otx2* misexpression in the rostral hindbrain repressed *Gbx2* expression and causes a posterior shift of the MHB (Broccoli et al., 1999). These observations suggest that an early event in formation of the MHB organizer is the establishment of the *Otx2* and *Gbx2* territories, followed by the activation of the other pathways (*Fgf8*, *Pax2*, *Wnt1*). The above described property of FGF8 protein to induce isthmus-like structures therefore probably reflects an Fgf8 function during a later, maintenance phase via a feedback loop involving *Otx2* and *Gbx2*, rather than a mechanism for early specification of the MHB primordium (Reifers et al., 1998; Lun and Brand, 1998; Liu et al., 1999; Martinez et al., 1999; Millet et al., 1999).

Mutants affecting the formation of the MHB in zebrafish showed that different pathways are involved in the early specification of the MHB primordium (reviewed in Rhinn and Brand, 2001). In the *acerebellar* (*ace*) mutant, which affects formation of the MHB and cerebellum, the *fgf8* gene is mutated (Reifers et al., 1998). In the *no isthmus* (*noi*) mutant, which affects formation of the midbrain, MHB and cerebellum, the *pax2.1* gene is mutated (Brand et al., 1996; Lun and Brand, 1998). Analysis of these two mutants showed that both genes are required during gastrulation stages for establishment of gene expression around the MHB, but that they are activated independently from each other in separate, adjacent stripes in the neural plate primordium for the anterior hindbrain (*fgf8*) and midbrain (*pax2.1*), respectively. From early somitogenesis-stages onwards, the expression domains of these genes overlap at the forming MHB territory and their expression becomes dependent on each other (Reifers et al., 1998; Lun and Brand, 1998). Neither in mouse nor in chick has *fgf8* expression been described at this early stage in the anterior hindbrain primordium; tentatively we suggest that another member of the Fgf family can perform the equivalent function in these species (see Section 3), such as Fgf4, which is expressed at the open neural plate stage in the chick neuroectoderm (Shamim et al., 1999).

To understand whether positioning of *pax2.1* and *fgf8* expression in their respective subdomains in the forming neural plate in zebrafish might depend on the interface between *otx* and *gbx* genes, we isolated and analyzed the zebrafish *gbx1* and *gbx2* genes and their interaction with *otx2* in zebrafish. *Gbx* genes are related to the *Drosophila unplugged* gene, which functions in development of the tracheal system and perhaps specific neuroblast sublineages (Chiang et al., 1995; Cui and Doe, 1995). In vertebrates, two subgroups can be distinguished by their aminoacid sequence (see also Fig. 1), the *Gbx1* and *Gbx2* subgroups (Chapman and Rathjen, 1995). *Gbx2* genes have been isolated from *Xenopus* (von Bubnoff et al., 1996), mouse (Bouillet et al., 1995), human (Lin et al., 1996) and chicken (Shamim and Mason, 1998; Niss and Leutz, 1998); furthermore, PCR analysis detected *gbx* genes in Australian lungfish (Longhurst and Joss, 1999) and sea urchins (Morris et al., 1997). Common to all vertebrate *Gbx2* genes studied so far is the expression at the MHB, suggesting that *gbx2*'s role in MHB formation is conserved in evolution. In contrast, little is known about *gbx1* genes; potential *gbx1* homologues have been cloned only as partial sequences in mouse (Frohman et al., 1993), chicken (Fainsod and Greunbaum, 1989), human (Matsui et al., 1993) and carp (Stroband et al., 1998), but so far no complete description of the temporal and spatial expression patterns is available.

Here we analyze the spatiotemporal expression patterns of the zebrafish *gbx2* and *gbx1* genes, and show that both genes are expressed at the MHB from early stages onwards. Our results extend a partial account of the *gbx2* expression pattern (Su and Meng, 2002). Furthermore, the analysis in *ace* (*fgf8*) mutants revealed that in zebrafish the activation of *gbx2* is strictly dependent on *fgf8* function, whereas the earlier activation of *gbx1* requires neither *fgf8* nor *pax2.1*. Thus, the highly dynamic spatiotemporal expression of the *gbx* genes, as well as the genetic dependence, both argue that this group of genes performs multiple distinct functions during development of the brain and other tissues.

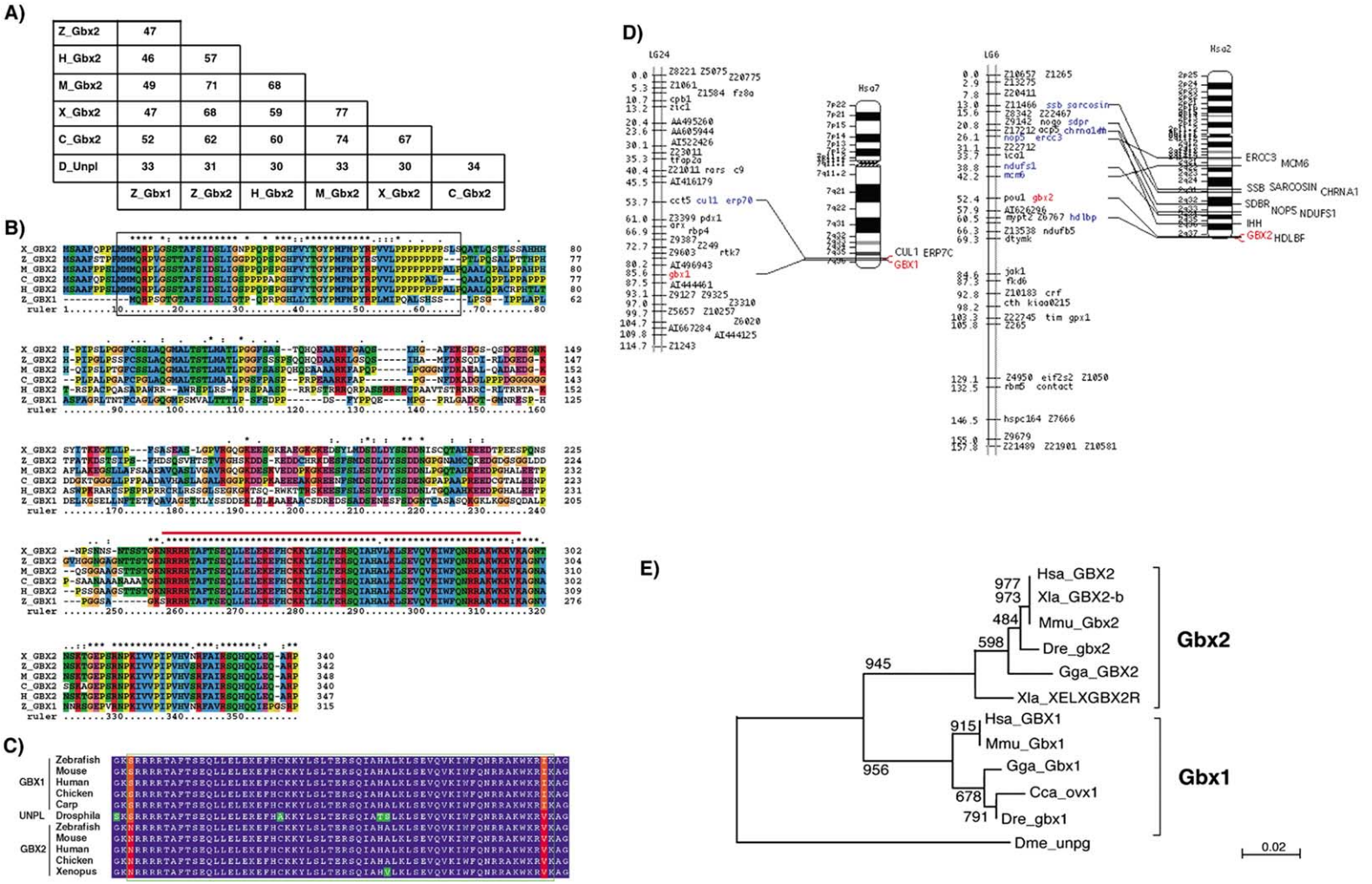

Fig. 1. Sequence comparison of the *Gbx1* and *Gbx2* genes. (A) Percentage sequence identity between different Gbx family members. (B) Sequence alignment of full length *Gbx2* genes; the black box outlines the N-terminal conserved region, which is enriched in prolines (yellow). The red bar marks the homeodomain. Stars show conserved aminoacids in all sequences; two points indicate chemically highly related aminoacids, one point chemically related aminoacids. (C) Sequence alignment of Gbx homeodomains; the green box marks the aminoacids of the homeodomain. Gbx proteins can be subdivided into class 1 and class 2 genes, depending upon their homeodomain sequence. A serine (S) or a arginine (N) at position 1 and an isoleucine (I) or a valin (V) at position 59 codes for Gbx1 and Gbx2, respectively. In-between the sequence of a putative ancestor, the *Drosophila unplugged* gene is shown, which contains a serine at position 1 and a valin at position 59. (D) *gbx1* and *gbx2* occupy syntenic map positions between zebrafish linkage groups 24 and 6 and human Hsa7 and Hsa2 chromosomes. Markers in support of synteny are shown in blue, and to the right of the human chromosomes. (E) Sequence alignments show that the zebrafish *gbx* genes are members of the two larger clades of vertebrate *Gbx* genes (see Section 4 for details).

2. Results

2.1. Cloning of the zebrafish gbx1 and gbx2 homologues

We isolated two putative *gbx* related cDNAs. One clone was identified during an in-situ hybridisation screen for genes with embryonic expression patterns. The other clone was isolated by screening a cosmid library for novel homeobox genes, and amplifying the cDNA for the predicted open reading frame by PCR. The predicted aminoacid sequence of both clones showed high homology to Gbx proteins (Fig. 1A). Alignments of the available Gbx sequences showed that the Gbx proteins can be subdivided into two classes based on diagnostic aminoacid substitutions at positions 1 and 59 within the Gbx homeodomain (Fig. 1B, C). Residue 1 is either a serine or an asparagine and residue 59 is either an isoleucine or valine (Chapman and Rathjen, 1995), in the Gbx1 and Gbx2 class, respectively. The homeodomain sequence of one clone contains a serine in position 1 and an isoleucine at position 59, identifying it as a *Gbx1* class gene, which we hence named *gbx1*. This is supported by a comparison of *gbx1* with all known *Gbx2* genes sequences: the aminoacid identity between the zebrafish Gbx1 protein and the Gbx2 protein from other species is around 52%, whereas the identity to various Gbx2 proteins is higher, ranging from 57 to 77% (Fig. 1A). We observed a conserved N-terminal portion between the zebrafish Gbx1 protein and the Gbx2 proteins (Fig. 1B, boxed region). We used blast search in order to check if this conserved N-terminal portion of the zebrafish Gbx1 and Gbx2 proteins can be found in either the mouse or human genome. We have identified a human aminoacid sequence showing 84% identity to the zebrafish Gbx-Box. This homologous region localises to the position on chromosome 7, where the human *Gbx1* gene maps. We have also identified a mouse aminoacid sequence showing 81% identity to the zebrafish Gbx-Box and this homologous region localises at the position on chromosome 5, where the mouse *Gbx1* gene maps. These findings suggest that *gbx* genes might generally share a distinctive N-terminal Gbx-Box that is conserved between the two family members.

The *gbx2* cDNA clone shows more than 64% aminoacid similarity with Gbx2 proteins in other species (Fig. 1A). The diagnostic aminoacids present in the homeodomain clearly assign the *gbx2* clone to the *Gbx2* class genes (Fig. 1C). We have so far not found additional members of the *Gbx* family. To further examine the relation between zebrafish and mammalian *gbx* genes, we have mapped the zebrafish *gbx1* and *gbx2* genes using a radiation hybrid panel and compared their position to that in mammals (Fig. 1D). The analysis reveals that both genes occupy areas of long-range synteny between the zebrafish and mammalian genomes, thus supporting the assignment of the *gbx1* and *gbx2* orthologies. A substantial portion of the long arm of human chromosome 2 (Hsa2q) is present in duplicate copies on zebrafish LG6 and LG9 (Amores et al., 1998; Postlethwait et al., 1998). LG6 contains at least eleven orthologues of Hsa2q genes including *gbx2*/*Gbx2*. Likewise, at least three genes occupying a very small portion of Hsa7 are linked on LG24 (Fig. 1D). The syntenic area is very extensive for *gbx2*, and slightly less so for *gbx1*. We suggest that a small inversion may have occurred in the vicinity of *gbx1* in either the teleost or mammalian lineage (Fig. 1D), as is frequently seen in overall syntenic regions between teleost and tetrapod genomes (Postlethwait et al., 2000). We conclude that conserved syntenies provide independent evidence for orthology assignments of these *gbx* sequences. The phylogenetic tree (Fig. 1E) shows that the vertebrate *Gbx* gene family has two main clades, *Gbx1* and *Gbx2*, and that each of the two zebrafish sequences falls into one of the two clades with high bootstrap support.

2.2. Embryonic expression of zebrafish gbx1

We investigated the temporal and spatial distribution of *gbx1* RNA by whole mount in-situ hybridisation (ISH). Expression of *gbx1* is first detected after the mid-blastula transition in a circular domain within the yolk syncytial layer (YSL), a cellular syncytium underlying the blastoderm (Fig. 2A–D). At 50% of epiboly, *gbx1* is activated in the upper blastoderm margin (Fig. 2C,D), but is downregulated in the shield of the embryo, a region which later gives rise to the zebrafish equivalent of Spemann's organizer. At the shield stage, prior to gastrulation, *gbx1* is downregulated in the YSL (Fig. 2E,F). The *gbx1* expression domain abuts the ntl/T expression domain, with an overlap of the two domains of around 2–3 cells (Fig. 2G) showing that *gbx1* is expressed in the upper part of the blastoderm margin. At the onset of gastrulation, the circular *gbx1* domain becomes progressively restricted to the dorsal part of the embryo, marking the caudal part of the neural plate (Fig. 2H,I). At 80% of epiboly, *gbx1* is expressed in a broad stripe in the caudal neural plate, and shows also a patchy expression in more posterior regions that later will give rise to the spinal cord (Fig. 2J). Between tailbud-stage and the 5-somite stage the broad *gbx1* stripe is subdivided into several smaller domains (Fig. 2K). The most anterior domain directly abuts with the *otx2* expression, demarcating the future MHB (see Fig. 3). This MHB domain becomes restricted to the dorsal part of the neural tube and starts to fade away at the 6–7-somite stage (Fig. 2M). Expression of *gbx1* is down-regulated in the medial cells of the MHB domain (Fig. 2M, arrow), and persists in a group of unidentified cells (Fig. 2M). At the 13-somite stage these unidentified cells are located in two stripes near the neural tube (Fig. 2O,P) adjacent to the position of the future MHB (Fig. 3H); this expression domain may correspond to the forming trigeminal placode. The expression persists in these cells up to 20 h of development and is then down regulated.

gbx1 is expressed very dynamically during hindbrain development. At 80% of epiboly it is expressed throughout the hindbrain primordium, but with the onset of

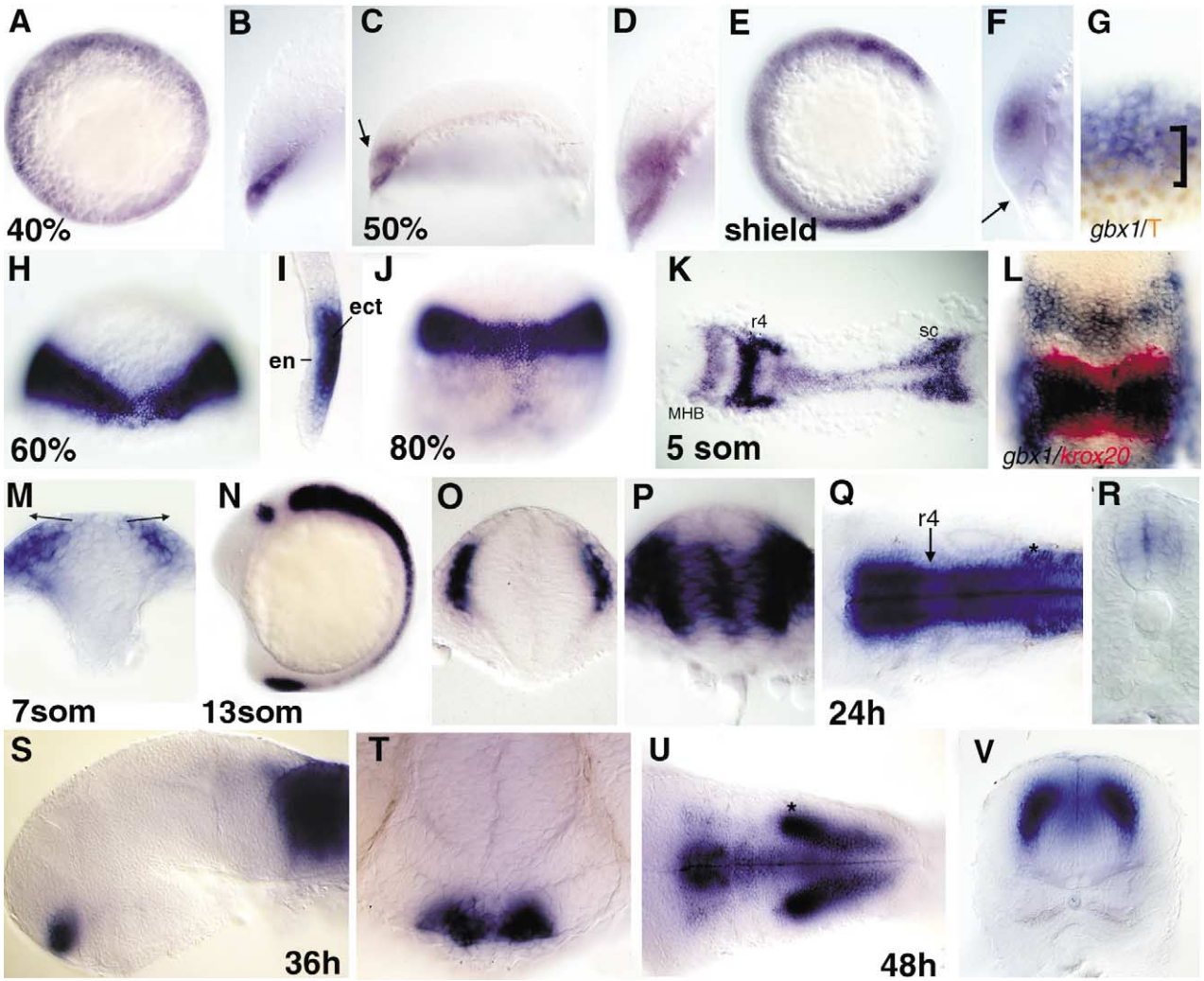

Fig. 2. Expression pattern of the *gbx1* gene by ISH. (A) Animal pole view at 40% of epiboly; *gbx1* is expressed in the yolk syncytial layer (YSL). (B) Cross-section showing *gbx1* expression in the YSL. (C) Cross-section, right is dorsal; at 50% of epiboly *gbx1* is downregulated in the most dorsal part of the embryo and is expressed also in the marginal blastoderm (arrow). (D) Close-up view of the embryo shown in (C). (E) Animal pole view with dorsal to the right, at shield stage; *gbx1* is not expressed in the future shield and the expression is downregulated in the YSL (F), arrow. (G) Close-up view of the marginal blastoderm showing the *gbx1* expression (ISH, blue) and the ntl/T protein (immunostaining, brown). An overlap of the two domains of around 2–3 cells is observed (clamp). (H) Dorsal view; after the onset of gastrulation *gbx1* is expressed in the prospective posterior neural plate and the cross-section (ect, ectoderm) (I) shows no expression in the newly involuting endomesoderm (en) (animal pole towards top). (J) Dorsal view; *gbx1* is expressed in a broad stripe in the hindbrain. The compact domain falls apart in the domains seen at the 5-somite stage (K) (sc, spinal cord; r4, rhombomere 4). (L) Double ISH of *gbx1* and *krox20*, which clearly identifies the strong hindbrain domain as r4. (M) Cross-section through the MHB domain at the 7-somite stage; the *gbx1* positive cells are absent in the dorsal MHB (arrows). (N) Lateral view; *gbx1* is expressed throughout the hindbrain and spinal cord at 13-somite stage. (0) Cross-section through the most anterior domain seen in (N); the two *gbx1* positive patches lie directly adjacent to the neural tube. (P) Cross-section through r3; *gbx1* is not expressed in the dorsal and ventral neural tube. (Q) Expression at 24 h in the hindbrain; expression is weaker in r4 (arrow). (R) Tail section at 24 h; *gbx1* is not expressed in the floor and alar plate. (S) Lateral and (T) ventral view at 36 h; a new *gbx1* domain is seen in the basal telencephalon above the optic recess. (U) Expression in putative hindbrain branchiomotor neurons in the hindbrain at 48 h, (V) cross-section at the level of nX; *gbx1* is strongly expressed in nascent neural cells, probably motorneurons of nX.

somitogenesis expression is strongly upregulated in rhombomere 4 (r4), as shown by double ISH with *krox20* (Oxtoby and Jowett, 1993), a marker for r3 and r5 (Fig. 2L). At 9-somite stage expression in the other rhombomeres is also upregulated and from 16 h of development onwards expression in r4 is weaker relative to the other rhombomeres. At 24 h *gbx1* is downregulated in r4 (Fig. 2Q arrow). Optical cross-sections through r3 (Fig. 2P) and the spinal cord (Fig. 2R) show that in the hindbrain/spinal cord *gbx1* expression is restricted to the intermediary part and excluded from the dorsal and ventral neural tube. At the13-somite stage two lateral domains can be detected near the neural tube at the level of r3 which may be head placodes (Fig. 2P). These cells are first detected at the 8-somite stage. At 48 h expression in the hindbrain is seen in two medial and two lateral groups of cells (Fig. 2U, asterisk) that probably correspond to branchiomotor neurons (compare Isl-1 staining in Chandrasekhar et al., 1997);

the cross-section at the level of the nucleus of the Xth nerve (Fig. 2V) shows that expression is not located at the ventricular surface, and therefore probably in nascent neurons of the forming mantle layer. Expression of *gbx1* in this area is already detected at 24 h, visible as two small lateral domains arising at a level posterior to the ear vesicle (Fig. 2Q, asterisk). At 30 h of development, *gbx1* is expressed also in the basal telencephalon in the area of the forming anterior commissure (Fig. 2S,T), just dorsal to the optic recess.

2.3. Relation of the gbx1/otx2 interface to MHB formation

Expression of *gbx1* begins much earlier in the developing neural primordium than *gbx2* and we therefore sought to determine in double ISH the relationship between *gbx1* and *otx2* expressing cells. From the onset of gastrulation onwards, *otx2* is expressed in the anterior neural plate, forming a posterior expression border at the MHB (Li et al., 1994; Mercier et al., 1995; Millet et al., 1996). At 60% of epiboly, the anterior border of *gbx1* expression directly abuts the *otx2* expression, with an overlap of the two domains of around 3–4 cells (Fig. 3A,B). This area of overlap has disappeared by 80% of epiboly, resulting in two sharply defined, directly adjacent domains (Fig. 3C–E). These observations suggest an early phase of establishment, with overlapping *gbx1* and *otx2* expression, followed by a later phase, where they may mutually repress each other. This boundary is maintained at later stages of development (Fig. 3F,G), until eventually *gbx1* is down-regulated at the MHB at the 6-somite stage; concommitant with down-regulation of *gbx1*, the boundary appears less sharp, in particular in the dorsal midline (Fig. 3H arrowhead).

Next we examined the position of the *gbx1/otx2* interface relative to MHB formation by comparing the expression of *otx2* and *gbx1* with that of *pax2.1*. Activation of *pax2.1* at the MHB is initially slightly patchy, and interestingly, activation occurs initially only within the *otx2* domain (Fig. 4A,B). The patches of expression then fuse to the typical wing-shaped *pax2.1* domain seen around 80–90% of epiboly which now stretches across the *otx2/gbx1* border (Fig. 4C,D). This observation is confirmed when the onset of *pax2.1* is studied relative to *gbx1* expression; *pax2.1* is clearly activated outside the *gbx1* expression domain (Fig. 4E). At 80% of epiboly *gbx1* is expressed posterior to *pax2.1*, with a few cells of overlap (Fig. 4G,H). Fig. 4I shows how subsequently the *gbx1* domain is split up into the subdomains seen at the 4-somite stage (Fig. 2K), but also how the overlap between *gbx1* and *pax2.1* continuously increases (Fig. 4H,J) from 1 to 2 cells at 80% of epiboly (Fig. 4H) to about 4–5 cells at the 3-somite stage (Fig. 4J). These results show that *pax2.1* is activated exclusively within the *otx2* domain, but becomes quickly expressed in the rostral *gbx1* domain. These double ISH of *pax2.1/gbx1* and *otx2/gbx1* indicate that the *otx2/gbx1* interface demarcates the region of the future MHB. The mechanism by

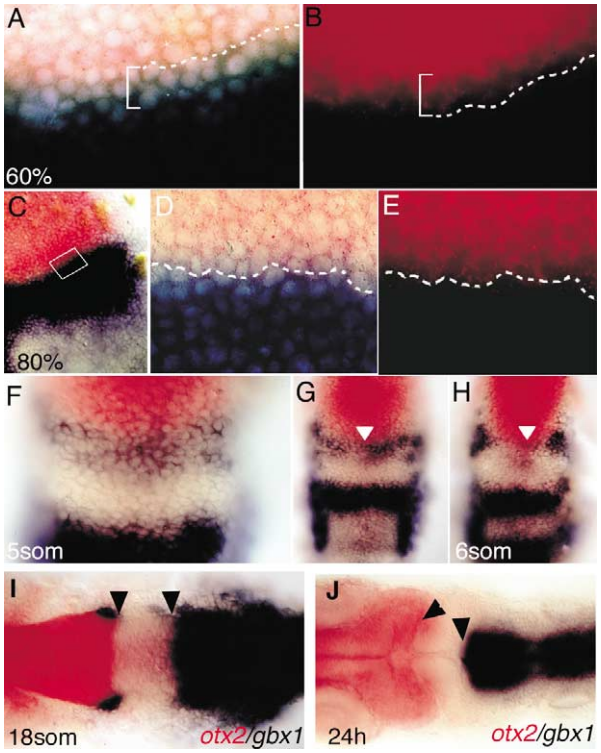

Fig. 3. *gbx1* expression relative to *otx2* expression. Shown are dorsal views, with anterior to the top; *gbx1* is stained in blue, *otx2* in red. (A,B) At 60% of epiboly the expression domains of *gbx1/otx2* overlap in a small row of 3 cells (clamp) (the white dashed line shows the limit of the *gbx1* expression domain (blue) in A and the limit of the *otx2* expression domain (red) in B). (C–E) At 80% of epiboly the border of the two domains is defined sharply; the higher magnification in (D,E) shows that there is no overlap between the *gbx1* and *otx2* domain (the white dashed line shows the limit of the *gbx1* expression domain (blue) in D and the limit of the *otx2* expression domain (red) in E). (F) The sharp *otx2/gbx1* border is unchanged at the 5-somite stage, and (G,H, arrowhead) the sharp posterior *otx2* expression is also kept up after the *gbx1* expression is downregulated at the MHB. (I) and (J) From mid-somitogenesis stages onwards a gap between the rostral *gbx1* and caudal *otx2* expression can be observed (arrowheads), that defines exactly the region where the morphological visible MHB fold will form.

which on the one hand the expression border between *otx2* and *gbx1* is maintained up to the 6-somite stage, and on the other hand overlap of *pax2.1* and *gbx1* increases between 80% to the 5-somite stage is unclear, but is likely to involve a mix of cell migration, proliferation and changes in gene expression.

The expression pattern of *gbx1* suggests that the primordium of the MHB, the area that later will form the morphologically visible fold, arises from an early *gbx1* positive field of cells that later becomes *gbx1* negative. The expression pattern at the 5-somite stage shows a defined *gbx1* positive band at the MHB, followed posteriorly by a gap of non-expressing cells, and then by the expression in r4 (Fig. 2K). At later stages, when the MHB domain starts to fade away (Fig. 2M), *gbx1* expression is upregulated also in more anterior rhombomeres, but expression does not touch the *otx2* domain (not shown). Double ISH with *otx2* and *gbx1* clearly shows that at mid-somitogenesis stages, there

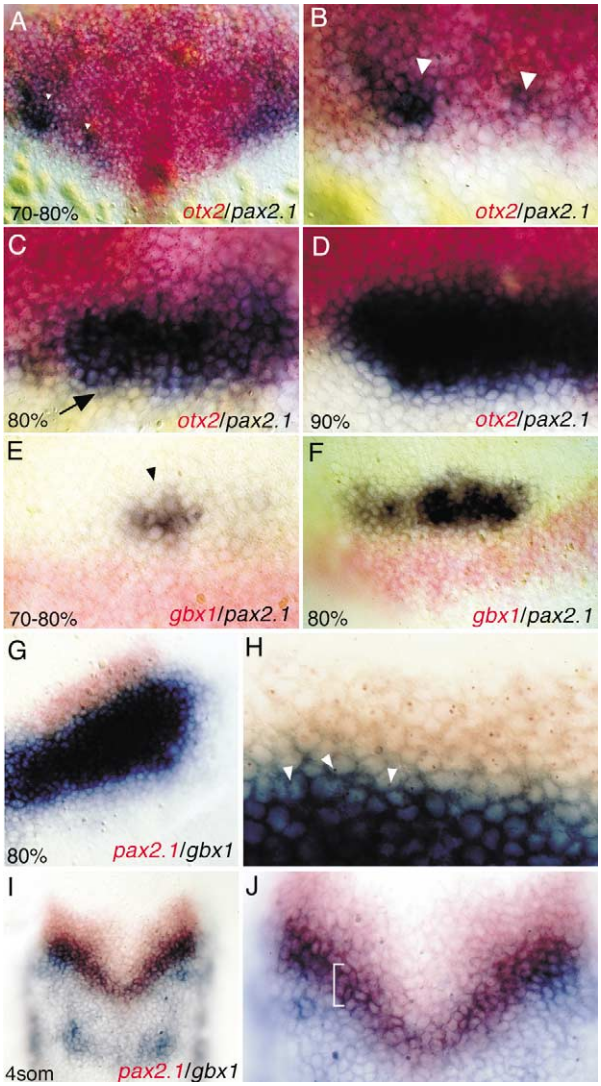

Fig. 4. Expression of *pax2.1* relative to *gbx1* and *otx2*. All embryos are shown from dorsal, with anterior to the top. (A) Onset of *pax2.1* expression (blue) in the *otx2* domain (red); the close-up in (B) shows, that *pax2.1* is activated in small patches (white arrowheads) within the *otx2* domain. (C) From 80% onwards, *pax2.1* becomes activated also posterior to the *otx2* domain (arrow), and at 90% (D) already a large *pax2.1* domain outside the *otx2* territory can be detected. (E,F) At 70–80% of epiboly *pax2.1* (blue) is activated outside the *gbx1* (red) domain (arrowhead); shown is a close-up view of the MHB domain of *gbx1*. (G–J) Double ISH of *pax2.1* (red) and *gbx1* (blue). At 80% a small overlap of *pax2.1*/*gbx1* positive cells can be detected (arrowheads in H); the arrowheads mark the nuclear *pax2.1* expression. (I,J) At the 4-somite stage, *pax2.1* and *gbx1* clearly overlap (clamp), whereas the *gbx1*/*otx2* border is maintained (Fig. 3).

is a prominent gap between the caudal limit of *otx2* expression and the rostral margin of the *gbx1* expression domain in the hindbrain (Fig. 3I), that is neither midbrain (*otx2* negative) nor completely hindbrain (*gbx1* negative). Double ISH with *krox20* shows that the *gbx1* expression anterior to r3 includes at least r2, and comparison with *EphA4*, a marker expressed in r1, r3 and r5 (Xu et al., 1994) at 24 h, revealed that very likely r1 is not expressing *gbx1* (data not shown). Observation of the MHB primordium in double-stained embryos throughout development shows that this is exactly the region where the MHB fold, including the cerebellum will form (Fig. 3I,J). This is particularly evident at 24 h in a double stained embryo with *otx2* and *gbx1*, where the fold occupies the *otx2*/*gbx1* negative territory (Fig. 3J). Therefore we propose that at least from mid-somitogenesis stages onwards, the MHB or isthmocerebellar primordium forms a distinct embryonic field giving rise to a separate brain subdivision sandwiched in between the midbrain and the hindbrain. This distinct embryonic field or brain subdivision is characterised by expressing neither *otx2* nor *gbx1*, and by expressing MHB specific markers such as *pax2.1* (and *pax5* and *pax8*, Pfeffer et al., 1998) and the zinc finger transcription factor *Bts1* (Tallafuss et al., 2001). This is consistent with r1 being a part of the isthmocerebellar primordium in zebrafish, and with studies in chick that suggested a contribution of r1 to formation of the cerebellum (Martinez and Alvarado-Mallart, 1989). It is from this region that the future morphologically visible MHB fold, including the cerebellum, will form, and we therefore speculate that these genes serve to outline the isthmocerebellar primordium.

2.4. Differential activation of gbx2 in distinct germ layers

Unlike *gbx1* in zebrafish and *Gbx2* in mouse, expression of zebrafish *gbx2* is initially not complementary to *otx2*. In zebrafish, *gbx2* transcripts are first detectable at 90% of epiboly as a patchy expression domain in two stripes at the level of the prospective hindbrain (Fig. 5A), thus at a distinctly later stage than *gbx1*. Optical cross-section through this area reveals that *gbx2* at its onset is only expressed in the endomesoderm (Fig. 5B). Shortly afterwards, at 90–100% of epiboly, *gbx2* then becomes activated also in the overlying neural ectoderm (Fig. 5D,H). The ectodermal domain is shifted anteriorly by several cell diameters relative to the endomesodermal domain (Fig. 5D, H). At 100% of epiboly, *gbx2* transcripts are in addition detected at the border of the neural plate in two longitudinal stripes, which are still connected to the medial neuroectodermal domain; several head placodes, including the otic placode, are thought arise from this area (Fig. 5C). Thus both endomesoderm and ectoderm activate *gbx2* in a position-specific manner.

2.5. Expression pattern of gbx2 in whole mount embryos

Double ISH of *gbx2* with *krox20* showed that at the 1-somite stage, the endomesodermal *gbx2* domain extends posteriorly up to the level of r5, whereas the ectodermal domain extends up to r3 (Fig. 5I,J). Comparison with *otx2* shows that anteriorly *gbx2* is adjacent to *otx2*, similar to *gbx1*, albeit at a much later stage (Fig. 5E). During the beginning of the segmentation period, the ectodermal *gbx2* domain sharpens and becomes more restricted to the region of the future MHB. Double ISH with *pax2.1* clearly showed

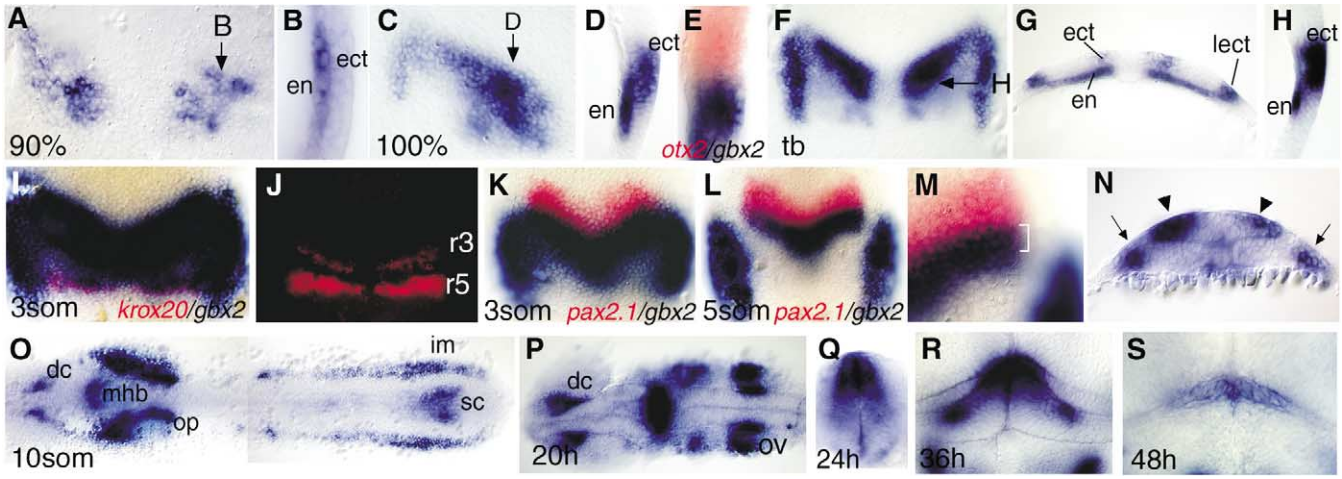

Fig. 5. Expression pattern of the *gbx2* gene by ISH. (A–D) Gastrula stage embryos, dorsal views and cross-sections, animal pole towards top. (A) At 90% *gbx2* is first expressed in two stripes in the endomesoderm (en), not in the ectoderm (ect), as shown in the cross-section in (B). (C) At 100% of epiboly the expression in the lateral neural plate can be detected (arrow). (D) The cross-section shows the ectodermal expression. (E) Double ISH with *otx2*; both domains are expressed adjacent to each other. (F) Tailbud stage all *gbx2* domains are visible. (G) Transverse cross-section showing the expression in the ectoderm, lateral ectoderm (lect) and endomesoderm and (H) cross-section. (I,J) Double ISH with *krox20*; the endomesodermal *gbx2* domains extends posteriorly up to r5. (K) *pax2.1* (red) overlaps with *gbx2* expression; (L) at the 5-somite stage the overlap is clearly visible, as shown in the close-up in (M, clamp). (N) Transverse cross-section through the tail of a 5-somite stage embryo. Expression in the spinal cord is marked with an arrowhead, the arrows mark the expression in the intermediate mesoderm. (O) Dorsal view of a 10-somite stage embryo (dc, diencephalon; op, otic placode; im, intermediate mesoderm) (P) Dorsal view at 20 h, with anterior to the left (dc, diencephalon; ov, otic vesicle). (Q) Cross-section through the MHB at 24 h; *gbx2* is expressed in a D/V gradient (R) Dorsal view of the MHB at 36 h, anterior to the top. (S) Dorsal view of the MHB at 48 h. The MHB expression is now restricted to the dorsal medial part.

that the *gbx2* expression is located in the posterior part of the MHB, overlapping with the *pax2.1* expression (Fig. 5K,L) similar to *gbx1*/*pax2.1* in Fig. 4. At 24 h of development, *gbx2* is expressed differentially along the dorso-ventral (DV) axis at the MHB (Fig. 5Q) and the dorsal views in Fig. 5R show that the expression is restricted to the medial part of the fold, extending ventroposteriorly into the cerebellar primordium. At 48 h the MHB domain is confined to the dorsal part of the fold and Fig. 5S shows that only the medial cells of the fold express *gbx2*, excluding the cerebellum.

During segmentation stages, *gbx2* is also expressed in the caudal spinal cord, in two lateral patches close to the tailbud (Fig. 5N) that later fuse at the dorsal midline (Fig. 5O); At the 10-somite stage, a new domain in the dorsal forebrain can be detected (Fig. 5O). We also observed *gbx2* positive cells located outside the neural tube in cells in/or near the otic vesicle (Fig. 5P).

At 5-somites, *gbx2* starts to be expressed in two lines in the lateral plate mesoderm (Fig. 5N,O) in a pattern very similar to genes that are known to be involved in hematopoesis, such as SCL or GATA1 (Liao et al., 1998; Thomson et al., 1998). Around the 18-somite stage, this expression domain is restricted to the area that will give rise to the intermediate cell mass, ICM, where the future blood cells will be formed. Interestingly, the expression in the ICM is downregulated by 24 h, but *gbx2* expression persists in the dorsal and ventral most trunk surface ectoderm, that will give rise to the apical ectodermal ridge (AER) of dorsal caudal and anal fins (data not shown). Expression of *gbx2* is also found in the developing retinal ganglion cells and in the ectodermal cells surrounding the developing lens (data not shown). Our data also confirm *gbx2* expression in the otic primordium/vesicle, as shown in tetrapods (Bouillet et al., 1995; von Bubnoff et al., 1996; Niss and Leutz, 1998). At the 2–3-somite stage, the lateral ectodermal domain separates from the medial domain (compare Fig. 5K and L) and increases dramatically in size. The domain splits into a posterior expression at the position of the ear placode and into an anterior domain near the neural tube. In the otic vesicle *gbx2* is expressed along the medial inner side, where the otic epithelium abuts the rhombencephalon (data not shown).

2.6. Onset and early expression of gbx1 is not affected in noi, ace and spg mutants

To determine where the *gbx* genes act in the genetic hierarchy controlling MHB development, we examined their expression in mutants affecting the formation of the MHB. Alleles of *no isthmus* (*noi*) are mutations in the zebrafish *pax2.1* gene (Brand et al., 1996; Lun and Brand, 1998), and the onset of *gbx1* expression is normal in homozygous *noi* mutants. From 80% of epiboly onwards, after the onset of *pax2.1* expression, no significant difference in *gbx1* expression is detected between wild-type (WT) and *noi* mutants up to the 5-somite stage (not shown). The *gbx1* expression at the MHB is downregulated in WT embryos at the 6–7-somite stage (Fig. 2M); in the *noi* mutant this dorsal MHB domain disappears somewhat earlier, at the 5–6-somite stage (Fig. 6B) and also the two *gbx1* positive cell clusters (Fig. 2N,O) could not be detected

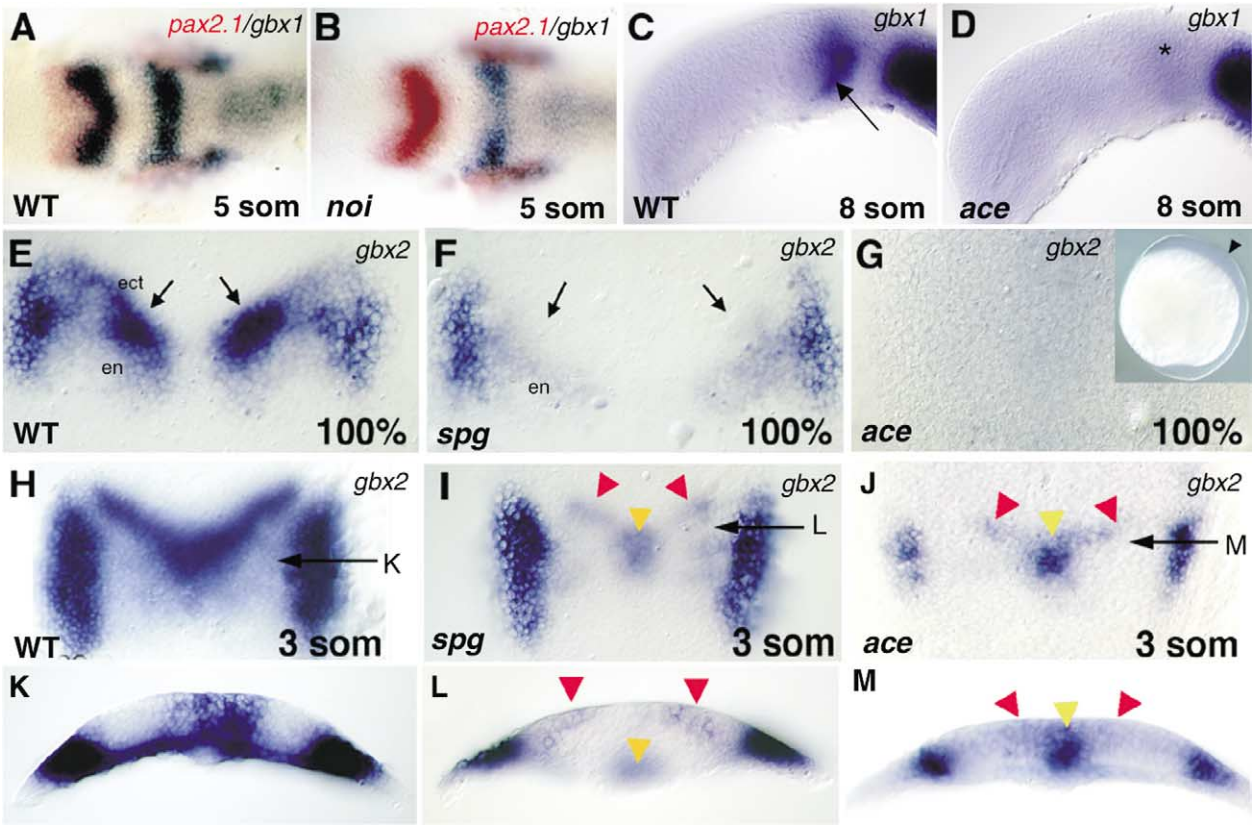

Fig. 6. Expression of *gbx1* and *gbx2* in *noi*, *ace* and *spg* mutants. (A,B) Dorsal views, anterior to the left, (C,D) lateral view, anterior to the left. (A) *pax2.1* (red) overlaps with the *gbx1* (blue) MHB expression; in (B) *noi* mutants the *gbx1* expression at the MHB is gone at 5 somites. (C,D) The lateral patches (arrow in C), which arise from the *gbx1* MHB domain, do not form in *ace* mutants (asterisk). (E,J) Shown are dorsal views, anterior to the top. (E–G) At 100% of epiboly *gbx2* is not expressed in the ectoderm (ect) in *spg* (F, arrows; en, endomesoderm) and *ace* mutants (G, arrowhead). (H–J) From 1 somite onwards, *gbx2* is reexpressed in the ectoderm, in three patches: in the medial neuroectoderm (yellow arrowhead) and in the lateral domains (red arrowheads). (K–M) show the cross-section through the embryo shown in (H–J), respectively; the lateral domains are migrating towards the dorsal midline.

at the 13-somite stage. At 24 h the hindbrain domain of *gbx1* is shifted a bit anterior in *noi* mutants, concommittant with the lack of MHB tissue (data not shown), similar to *acerebellar* (*ace*) mutant embryos, which lack *fgf8* function (Reifers et al., 1998). The onset and early expression of *gbx1* is normal in *ace* mutants, but at midsomitogenesis, the dorsal MHB domain and later also the two patches lateral to the MHB are absent (Fig. 6C,D, asterisk). At 24 h, due to the lack of MHB tissue, *gbx1* expression in the hindbrain is shifted anteriorly also in *ace* mutants (data not shown). The observation that in *noi* and *ace*, two mutations that affect MHB formation at early somitogenesis stages, the *gbx1* domain lateral to the MHB (see Fig. 2M) is never seen, is consistent with our suggestion that cells in this domain might derive from the MHB expression domain seen at the 5–7-somite stage. Alternatively, proper specification of the MHB domain might be a prerequisite to induce this population of cells in neighboring placodal ectoderm. In contrast, in mutations, in the *pou2* gene (Schier et al., 1996; Belting et al., 2001; Burgess et al., 2002; Reim and Brand, 2002) cause no significant difference in *gbx1* expression between WT and mutant embryos at early stages.

In summary, expression of *gbx1* is not affected in *noi*, *ace* or *spg* mutants at early stages when the MHB is established, suggesting that *gbx1* acts upstream of these genes.

2.7. Onset of gbx2 expression is dependent on fgf8 signaling

In contrast to *gbx1*, our analysis of *gbx2* expression in the MHB mutants shows that *gbx2* is dependent on *spg* (*pou2*) and *ace* (*fgf8*) function. At 100% of epiboly, *gbx2* expression is seen only in the endomesodermal and in the presumptive otic domains of *spg* mutants (Fig. 6E,F) (see also Reim and Brand, 2002). At the 3-somite stage, the *gbx2* positive ectodermal patches are visible more clearly and are shifted towards the dorsal midline, presumably due to the neural keel condensation movements taking place at this time (Fig. 3H,I). Around the 10-somites, the *gbx2* domain at the MHB is absent. At 24 h of development the MHB domain is still lacking, whereas the other domains are unchanged compared to WT embryos (data not shown).

Onset of *gbx2* expression is also affected in the *ace* mutant, albeit in a different way (see also Reim and Brand, 2002). In *ace* mutants, expression is already absent at 90% of epiboly

(Fig. 6E,G), and does not appear until the 2-somite stage, when weak expression becomes detectable in the mutants in the presumptive otic primordium and in dorsal midline; both the expression in the MHB and in the presumptive otic primordium are strongly decreased at the 2-somite stage (Fig. 6H,J). The cross-section in Fig. 6M shows that *gbx2* is reexpressed in *ace* only weakly in the ectoderm, and not at all in the endomesoderm. Also at 24 h, no *gbx2* expression can be detected at the MHB in *ace* mutants, whereas the other *gbx2* domains are not or only mildly affected in *ace* mutants (data not shown). Therefore we conclude that *fgf8* signaling is required for the onset of *gbx2* expression in the MHB, in the underlying endomesoderm and in the presumptive otic placode, whereas for expression in other *gbx2* domains *fgf8* is less crucial. In *noi* mutant embryos the onset of *gbx2* expression is not affected, and it is expressed essentially as we have described for *fgf8* in *noi* mutants at later stages (Lun and Brand, 1998, and not shown). These observations suggest, together with the results in *ace* mutants, that Fgf8 is intimately involved in regulating *gbx2*.

The observation that *gbx2* is expressed both in the endomesoderm and the overlying ectoderm raised the question where *fgf8* is needed to activate *gbx2* expression. We therefore examined if *fgf8* itself is expressed in the endomesoderm underlying the forming MHB. Cross-sections show that at 70% of epiboly, *fgf8* is expressed in both the endomesoderm and the overlying ectoderm, but expression is extinguished in the endomesoderm by the 90%-tailbud stage (Fig. 7A–D, arrows). Endomesodermal cells derive by involution from the blastoderm margin, and

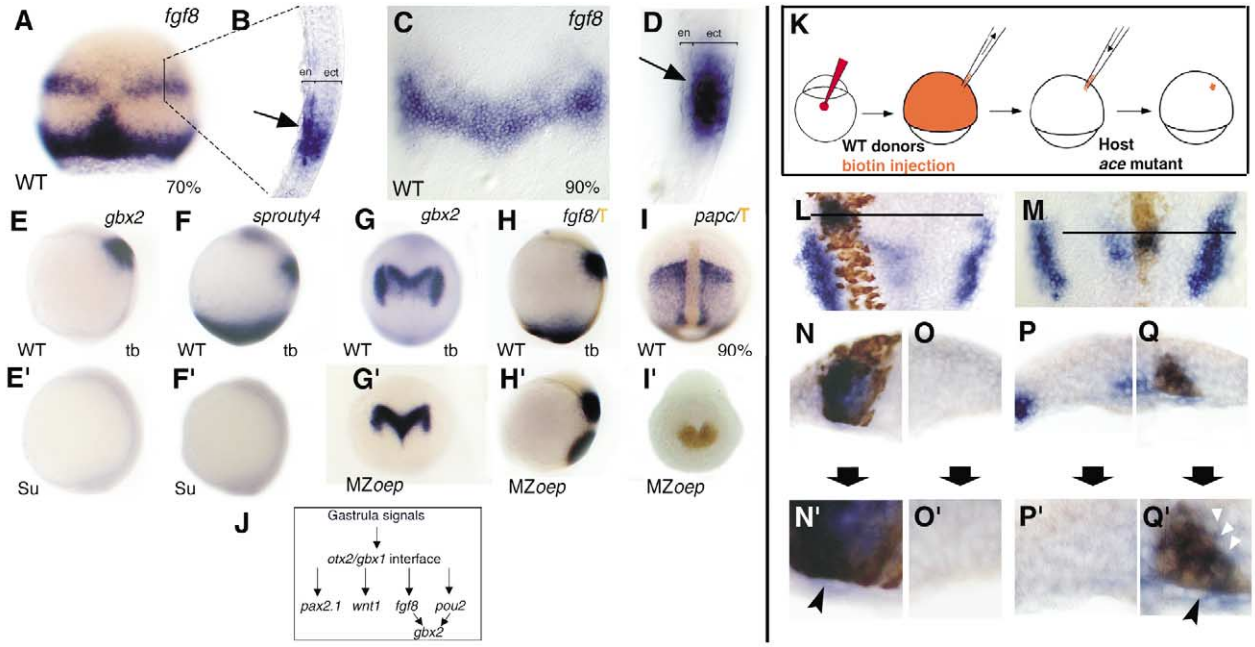

Fig. 7. *gbx2* expression in the ectoderm and endomesoderm requires ectodermal Fgf8. (A–D) Expression of *fgf8* at late gastrula stages in the ectoderm (ect) and underlying endomesoderm (en). (A) At 70% of epiboly, *fgf8* is expressed in the prospective hindbrain neuroectoderm, abutting posteriorly to the prospective MHB. (B) The cross-section of the embryo in (A) shows, that *fgf8* at its onset is also expressed in the underlying endomesoderm (en, arrow). (C) Dorsal view, anterior to the top; at 90% the *fgf8* domain looks very similar to the *gbx2* domain (compare to Fig. 5), which reflects the dependency of *gbx2* on *fgf8* expression. (D) Cross-section through the *fgf8* domain at 90% of epiboly, at the onset of *gbx2* expression; *fgf8* is no longer expressed in the endomesoderm, but remains on in the ectoderm. (E,E′,F,F′) *gbx2* expression in SU5402 treated embryos. (E) *gbx2* expression at tailbud stage in non-treated embryos. (E′) In embryos treated with SU5402 from 70% of epiboly to tailbud, the *gbx2* expression is abolished. (F) *sprouty4* expression at tailbud in non-treated embryos. (F′) In embryos treated with SU5402, the expression of *sprouty4*, an Fgf target, is abolished showing that the inhibition of Fgf signaling was efficient. (G,G′,H,H′,I,I′) *gbx2*, *fgf8* and *papc* expression in MZ*oep* embryos. (G,G′,I,I′) posterior view, (H,H′) lateral view. (G) *gbx2* expression in WT embryos at tailbud-stage (G′) *gbx2* is expressed in the ectoderm in MZ*oep* embryos where the underlying endomesoderm is absent (I′). (H) *fgf8* expression in a WT embryo at tailbud-stage and in MZ*oep* embryos (H′). (I) *papc* is expressed in lateral mesoderm (blue) is completely absent from axial mesoderm where ntl/T immunostaining is detected (brown) in a WT embryo at tailbud stage. (I′) In MZ*oep* embryos no *papc* staining is detected showing the absence of the underlying endomesoderm. Only ntl immunostaining is detected in the tailbud. (J) Regulation of *gbx* genes in zebrafish. During gastrula stages, three parallel pathways (Pax, Wnt and Fgf) are activated around the *otx2/gbx1* interface in response to patterning signals. Towards the end of gastrulation, *spg* (*pou2*) expression refines to the MHB territory. At the end of gastrulation, *ace* (*fgf8*) and *spg* (*pou2*) in turn are required to activate *gbx2*. (K) Schematic drawing of the transplantation procedure. Transplantations of biotin-labeled WT donor cells into *ace* host embryos were done at shield stage. (L,M) Dorsal view, anterior to the top. *gbx2* expression can be rescued in a host embryo (*ace*) transplanted with WT cells and processed for ISH and for detection of the biotin lineage tracer in the transplanted WT cells (brown). The line marks the level of the cross-section shown in (N,O) and (P,Q). (N,O) Cross-section of the embryo shown in (L) and (P,Q) cross-section of a second chimaeric embryo shown in (M) with a similar clone. *gbx2* expression is rescued in the transplanted cells, but also in the host mutant cells (white arrowhead in Q′) situated close to the transplanted cells. Other cells that are only brown lie outside the normal *gbx2* expression domain. (N′,O′) Higher magnification of the sections shown in (N,O). (P′,Q′) Higher magnification of the sections shown in (P,Q). Importantly, *gbx2* expression is also rescued in the endomesoderm (N′,Q′) (arrowhead) where no transplanted WT cells are detected. (O) cross-section of the contralateral (control) side of the embryo shown in (L) and (P) cross-section of the contralateral (control) side of the embryo shown in (M). No expression of *gbx2* is detected in the ectoderm and endomesoderm in the absence of WT cells in the host *ace* embryo.

therefore express *fgf8* also at earlier stages (e.g. shield stage). To test whether their previous location in the blastoderm margin allows them to somehow 'remember' to activate *gbx2* expression at 90% epiboly, we treated wild-type embryos from 70% epiboly onwards, i.e. shortly before activation in the endomesoderm occurs, with SU5402, an inhibitor of Fgf signaling (Mohammadi et al., 1997). We find that this treatment abolishes the onset of *gbx2* expression in all treated embryos in both germlayers (Fig. 7E,E′). Control ISH with the Fgf8-target gene *sprouty4* (Fürthauer et al., 2001) shows that the inhibition was complete (Fig. 7F,F′). These findings show that Fgf8 signaling is necessary specifically between 70 and 90% of epiboly for activation of *gbx2* expression in both the endomesoderm and ectoderm.

To examine in which germlayer *fgf8* expression is needed for *gbx2* activation, we transplanted WT cells at the shield stage into the prospective hindbrain ectoderm of *acerebellar* (*fgf8*) mutants which normally lack *gbx2* expression, and allowed the resulting chimaeric embryos to develop until the tailbud stage, the time when *gbx2* would normally be activated in wild-type embryos (Fig. 7K). As expected, the WT cells were able to express *gbx2* in the *ace* mutant ectoderm (Fig. 7L,M). *gbx2* is also induced in immediately neighboring *ace* cells that lie within the normally *gbx2*-positive band (Fig. 7Q′). These cells are not far away from the Fgf8 source, an observation which is in agreement with the data that Fgf8 target genes, like *sprouty4* and *gbx2*, have their expression domain closely overlapping with the *fgf8* expression domain (compare Fig. 7E,F,H; Fürthauer et al., 2001). In such chimaeric embryos, WT cells located in the ectoderm, labeled in brown, were also able to rescue the mesendodermal expression of *gbx2* in unlabeled homozygous mutant host cells, as confirmed by cross-sections at the level of the primordial hindbrain (Fig. 7N′–Q′). Thus, normal *fgf8* function is required in the ectoderm to allow *gbx2* expression in the underlying endomesoderm of late gastrula-stage embryos, revealing a novel Fgf8-dependent signaling event. Note, however, that this signaling event is not necessarily direct, because Fgf8 might activate another signaling protein in the ectoderm which in turn would activate endomesodermal *gbx2* expression.

We next examined the role of the endomesoderm, which transiently expresses *fgf8*, on the onset of *gbx2* in the overlying ectoderm. Maternal Zygotic one-eyed-pinhead (MZ*oep*) mutants are unresponsive to Nodal signaling and show severe disruption of endomesodermal development (Gritsman et al., 1999). Markers for endoderm, notochord, prechordal plate, paraxial mesoderm intermediate mesoderm and lateral mesoderm are not expressed in the head and trunk of MZ*oep* mutants (one example Fig. 7I,I′; Gritsman et al., 1999). Thus the ectoderm of MZ*oep* mutants is never exposed to the transient *fgf8* expression observed in the endomesoderm at 70% of epiboly (Fig. 7B) and is only exposed to the ectodermal *fgf8* expression which is normal in MZ*oep* embryos (Fig. 7H,H′). *gbx2* is expressed in MZ*oep* mutants although signaling from the endomesoderm is absent (Fig. 7G,G′). We conclude that Fgf8 expression in the endomesoderm is not required for the expression of *gbx2* in the ectoderm.

Together our findings demonstrate that Fgf8 signaling is required within the ectoderm for ectodermal *gbx2* expression, and that Fgf8 signaling or secreted targets of Fgf8 can signal vertically to the endomesoderm to activate and/or maintain *gbx2* in this layer. Our analysis does not support an involvement of the transient *fgf8* expression in the endomesoderm in the onset of *gbx2* expression in the ectoderm. The function of *gbx2* in the mesendoderm remains to be addressed.

3. Discussion

We have isolated and described the spatiotemporal activity of *gbx1* and *gbx2* and presented a detailed account of the expression of these genes and their functional context in particular during development of the midbrain–hindbrain territory; additional expression data are deposited in the ZFIN database (www.zfin.org). These genes are likely to function in this area in a complex fashion, as evidenced by their highly dynamic expression patterns. Our functional studies using the *noi*, *spg*, and *ace* mutants, as well as Fgf inhibition and transplantation experiments, clearly distinguish a likely *gbx1* function upstream of the genetic cascade acting in MHB development, from that of *gbx2* acting downstream of Fgf8 signaling and of *spg* (*pou2*) (Fig. 7J). Our data also suggest additional *gbx* gene functions at later stages of MHB development. Studies in *acerebellar* (*fgf8*) mutants and, in embryos after Fgf signaling has been blocked pharmacologically and transplantation studies reveal a novel requirement for Fgf8 signaling from the ectoderm to activate *gbx2* expression in the underlying mesendoderm. Apart from the general involvement of *gbx* genes in MHB development reported also in other vertebrates, these results stress that there are some important differences in the likely function of these genes in zebrafish, presumably reflecting the differential evolution of this gene family among vertebrates.

3.1. The zebrafish contains two members of the gbx gene family

Gbx2 genes have been isolated from different vertebrates, including chicken, human, mouse and *Xenopus* (Chapman and Rathjen, 1995; Lin et al., 1996; von Bubnoff et al., 1996; Niss and Leutz, 1998; Shamim and Mason, 1998), and all genes, including the zebrafish *gbx2*, show an overall high sequence similarity of more than 68% (see Fig. 1A). All Gbx2 proteins in addition show the diagnostic aminoacids in the homeodomain (Chapman and Rathjen, 1995), which clearly puts zebrafish *gbx2* into the *Gbx2*

subgroup. This notion is further supported by the conserved genomic organisation of zebrafish *gbx2* compared to the cognate mouse (Chapman et al., 1997) and human (Lin et al., 1996) *Gbx2* genes, including synteny of the chromosomal regions, and the results of our cladistic analysis. The expression patterns of *gbx2* in zebrafish and other vertebrates are overall conserved, with some important differences. Similar to zebrafish *gbx2*, the *Xenopus*, mouse and chicken *Gbx2* homologues are first detected during gastrulation and are later expressed in the anterior hindbrain, at the prospective MHB, the most prominent expression domain common to all *Gbx2* genes. In addition, the expression in the otic vesicle is present in all species. Similar to the mouse and chicken *Gbx2* gene, zebrafish *gbx2* is expressed at its onset in the endomesoderm and ectoderm, while *Xgbx2* expression was found only in the ectoderm (von Bubnoff et al., 1996). Both *Xgbx2* and zebrafish *gbx2* are expressed in the epidermal ectoderm, whereas in mouse and chicken no such expression could be observed (Shamim and Mason, 1998; Bouillet et al., 1995). Zebrafish *gbx2* is also expressed in regions not described so far in other species, for instance the transient expression in the lens ectoderm, which suggests an involvement in lens formation.

Gbx1 genes have been cloned in carp, human, mouse and chicken (Stroband et al., 1998; Fainsod and Gruenbaum, 1989; Matsui et al., 1993; Frohman et al., 1993), but so far only partial sequences have been reported, and a complete description of the spatiotemporal expression pattern was lacking in vertebrates. Based on sequence comparison, chromosomal synteny and cladistic analysis, zebrafish *gbx1* is clearly a member of the *Gbx1*-class of genes. Nevertheless, the early zebrafish *gbx1* expression pattern shares an important feature with the early *Gbx2* expression in mouse: both genes are expressed at the onset of gastrulation in the forming posterior neural plate, and directly abut the *Otx2* expression at the region of the prospective MHB. We have recently isolated a mouse *Gbx1* gene that is expressed similar to the zebrafish gene, but not in the forming posterior neural plate (Rhinn et al., 2003). At later stages, zebrafish *gbx1* is expressed predominantly in the hindbrain and spinal cord, whereas the mouse *Gbx2* is expressed in a highly dynamic pattern in various tissues, more similar to the zebrafish *gbx2*. It will be interesting to determine whether mouse or other vertebrate *Gbx1* homologues are activated in a similar way as in zebrafish. The carp *gbx1* homologue, called *ovx1* (Stroband et al., 1998), is indeed expressed similarly to zebrafish *gbx1*, but because zebrafish and carp are closely related as cyprinids, this must not necessarily reflect the situation in other vertebrates.

3.2. N-terminal conserved sequences within the Gbx genes may be required for transcriptional activation

Unexpectedly, the sequence comparison between the Gbx proteins revealed a stretch of 50 aminoacids in the N-terminal part that is highly conserved among the Gbx2 proteins (95% of identity), but also when compared with the zebrafish Gbx1 sequence (90% identity). This suggests that in addition to the conserved homeodomain an additional, conserved 'Gbx-box' is present at the N-terminus of Gbx proteins; indeed this sequence is also present in the human and mouse *Gbx1* genes (not shown). The Gbx-box sequence is highly enriched in proline residues (30% proline); such regions have been implicated as transcriptional activators (Gerber et al., 1994), raising the possibility that the N-terminal Gbx-box functions similarly in transcriptional activation. An attractive possibility is that the conserved Gbx-box might allow a *Gbx* specific, conserved interaction with the transcriptional machinery. Interestingly, a polymeric repeat of 4–9 prolines is present in all Gbx2 proteins (Fig. 1); apart from its suggested function in transcriptional regulation, expansion or contraction of such homomeric repeats is often associated with functional 'disease' mutations, similar to trinucleotide expansions seen in Huntington's disease (Lin et al., 1996); however, so far no specific mutations affecting this proline repeat have been reported. This proline stretch is reduced to one aminoacid in zebrafish Gbx1, which may reflect a functional difference to Gbx2 proteins in terms of transcriptional activation and regulation.

3.3. Expression of gbx1 during early development

The first transcripts of *gbx1* RNA are detected in the yolk syncytial layer (YSL, Kimmel et al., 1995). The YSL may function as the fish equivalent of the Nieuwkoop center, in that translocation of activated maternal determinants into the dorsal YSL may lead to the formation of an 'organizer-inducing-center' (Koos and Ho, 1998). Consistent with this function, various organizer-related genes are expressed in the dorsal YSL, including zebrafish *nodal related 2*, *bozozok* and *mixer* (Erter et al., 1998; Yamanaka et al., 1998; Fekany et al., 1999; Alexander et al., 1999). Increasing evidence suggests that the YSL and its mouse cognate structure, the visceral endoderm, are involved in D/V and antero-posterior (A/P) patterning of the overlying epiblast, as suggested by the zebrafish *hex* or *nieuwkoid/dharma* expression (Beddington and Robertson, 1998; Ho et al., 1999; Koos and Ho, 1998; Yamanaka et al., 1998). Zebrafish *gbx1* is exclusively expressed in the marginal YSL and becomes excluded from the most dorsal part at 40–50% of epiboly, which makes a function for *gbx1* in organizer function itself less likely. More likely, *gbx1* could be involved in correct specification of posterior fates in the overlying marginal blastoderm (the future endomesoderm), possibly via *wnt8*, a molecule expressed in the YSL and known to be required for mesoderm formation and posteriorisation of the neural plate (Kelly et al., 1995; Erter et al., 2001; Levken et al., 2001). However, gain- and loss-of-function analysis of *gbx1* specifically in the YSL does not cause a detectable phenotype (M.R. and M.B., manuscript in preparation),

leaving the function of *gbx1* expression in the YSL so far unclear.

3.4. The role of gbx genes in the development of the midbrain–hindbrain boundary region

The function of *Gbx2* in MHB development has been studied in mouse and other vertebrates (Wassarman et al., 1997; King et al., 1998; Tour et al., 2002; Martinez-Barbera et al., 2001; Li and Joyner, 2001; Li et al., 2002). Loss-of-function analysis of *Gbx2* in mice showed that *Gbx2* is required for proper development of the MHB (Wassarman et al., 1997; Li et al., 2002). Expression at the MHB in *Xenopus* (von Bubnoff et al., 1996) and chicken (Shamim and Mason, 1998) also suggests an important role for *Gbx2* in MHB formation. Our results show that in zebrafish *gbx1* and *gbx2* are expressed at the MHB from early stages onwards as well, albeit with an unexpected complexity that suggests an involvement at multiple regulatory steps. Previous analysis of MHB formation in zebrafish showed that the *pax2.1* (Lun and Brand, 1998) and *fgf8* (Reifers et al., 1998) genes are required for proper MHB formation. The onset of expression of these genes at the MHB occurs during gastrulation, at 80 and 70% of epiboly, respectively. Unlike in mice, *gbx2* is expressed only later, at 90% of epiboly, after the onset of *pax2.1* and *fgf8* in the anterior hindbrain. This later onset of expression relative to *pax2.1* and *fgf8* suggests a later function for zebrafish *gbx2* than for *pax2.1* and *fgf8*. Such a downstream function is consistent with our observation that already at its onset, *gbx2* expression in zebrafish completely depends on *fgf8* function in the MHB and the otic primordium (Fig. 7), and on the activity of *spg* (*pou2*) that is required to mediate competence to respond to Fgf8 (Fig. 6; Reim and Brand, 2002; Burgess et al., 2002). Work in mice and chick suggests a similar, but not identical hierarchy: in these species, *Gbx2* expression precedes *Fgf8* expression in the neuroectoderm, suggesting that for the activation of *Gbx2* genes other than *fgf8* must be involved. However, *Fgf8* is activated in chick and mice at a later stage relative to other MHB genes, and not throughout the anterior hindbrain. Nevertheless, Fgf8 can activate *Gbx2* expression when beads are implanted ectopically (Liu et al., 1999; Martinez et al., 1999), suggesting that Fgf8 or an Fgf8-like factor acts, directly or indirectly, upstream of *Gbx2* in mice and chick as well. Interestingly, the *Drosophila* homologue of *Gbx2, unplugged*, is required for formation of the tracheal branches that penetrate the fly CNS (Chiang et al., 1995), a process that also depends on *Fgf* gene function (Sutherland et al., 1996). These observations provide evidence for an evolutionarily conserved relationship between *fgf8* and *gbx2*.

Following up on the observation that *gbx2* is activated both in the endomesodermal and in the overlying ectodermal germ layer, we discovered a novel signaling event between these germ layers that involves Fgf8. At the stage when *gbx2* is activated, *fgf8* is expressed in both germ layers, and *gbx2* expression fully depends on Fgf8. Consistent with this notion, we find that blocking of Fgf-signal reception with SU5402 inhibitor shortly before the onset of expression abolishes expression of *gbx2* and *sprouty4*, *erm* and *pea3*, as Fgf8 target genes (Fürthauer et al., 2001; Raible and Brand, 2001). In such embryos, both germlayers lack *gbx2* expression, because Fgf8 is required in the ectoderm at this stage (Fig. 7; Reim and Brand, 2002). Theoretically, either vertical signaling between the ectoderm to the underlying endomesoderm, or signaling within each germ layer could account for the onset of *gbx2* expression. Based on the analysis of MZ*oep* mutant embryos, which lack the underlying endomesoderm, we conclude that *fgf8* expression in the endomesoderm at 70% is not required for ectodermal *gbx2* expression. Furthermore, our transplantation experiments argue that Fgf8 *is* required in the ectoderm for activation of *gbx2* in the underlying endomesoderm, although it is still unclear if this is a direct signaling event. Onset of *gbx2* expression occurs slightly earlier in the underlying endomesoderm, and the ectodermal and endomesodermal *gbx2* domain do not overlap exactly, raising the possibility that both domains might even be independently activated by other signals during a brief period that we have not detected. The analysis of *spg* (*pou2*) mutants has provided support for a direct influence of Fgf8 from the ectoderm, because in these mutant embryos, expression of only the ectodermal *gbx2* expression is affected, whereas expression in the endomesoderm is activated normally. The gene that is inactivated in *spg* mutants, *pou2*, is specifically expressed in the ectoderm at this stage, and is required to endow cells with the abilitiy to respond to Fgf8 specifically in the neuroectoderm (Reim and Brand, 2002). Although the *spg* mutants eventually loose ectodermal *fgf8* expression, they express *fgf8* transiently in the ectoderm (Reim and Brand, 2002), which could explain their ability to activate endomesodermal *gbx2* expression.

In mouse, the onset of *Gbx2* expression occurs when gastrulation starts, at E6.5-E7, before the onset of *Fgf8*, *Pax2* and other genes that are expressed at the MHB (Bouillet et al., 1995; Wassarman et al., 1997; Millet et al., 1999; Martinez-Barbera et al., 2001; Li and Joyner, 2001). In zebrafish, *gbx2* is apparently expressed too late to fulfill the same early function as *Gbx2* does in mouse. This difference in the temporal activation of *gbx2* between zebrafish and mouse or chicken suggests that in zebrafish, *gbx1* may perform the equivalent function to mammalian *Gbx2* upstream of the MHB genetic cascade. So far, no complete expression pattern of *gbx1* has been described in other species; in mouse, the expression has been reported to occur in restricted regions of the forebrain at E11,5 (Frohman et al., 1993), whereas we have found that murine *Gbx1* is expressed in other part of the CNS and outside, we have not observed any expression in the early neural plate (Rhinn et al., 2003). The chicken *Gbx1* homologue, *CHox7*

(Fainsod and Gruenbaum, 1989), is expressed from blastoderm stages onwards, but its spatial and temporal localisation is unknown, as is true for human *Gbx1*. In zebrafish, *gbx1* is expressed already at the beginning of gastrulation in the prospective posterior neural plate, and fate mapping (Woo and Fraser, 1995) indicates that this area gives rise to the primordia of hindbrain and spinal cord. Anteriorly, *gbx1* expression initially overlaps with *otx2* by about 3–4 cells, and then sharply abuts the *otx2* domain, long before the onset of *pax2.1* or *fgf8*. As shown in Fig. 3, this sharp boundary between *gbx1*/*otx2* forms between about 60 and 80% of epiboly, which therefore most likely corresponds to the time when mutually repressive interactions between *otx2* and *gbx1* could sharpen the boundary. In mice, misexpression of *Otx2* and *Gbx2* during later segmentation stages can result in shifting of the MHB organizer (Broccoli et al., 1999; Millet et al., 1999), but these genes have a common expression boundary already during gastrulation stages, and if mutually repressive interactions are important in normal development, they should take place already during the gastrulation period (see also Rhinn and Brand, 2001, for further discussion). Our observations on the sharpening of *otx2* and *gbx1* between 60 and 80% epiboly identify the relevant period during which mutually repressive interactions are likely to contribute to MHB development in zebrafish. Consistent with a *gbx1* function upstream of the MHB cascade, we find that *gbx1* expression at this stage is not affected in *noi*, *ace* or *spg* mutants. Moreover, loss- and gain-of-function experiments with *gbx1* support the importance of this regulatory event (M.R., K.L. and M.B., manuscript in preparation).

3.5. A paralogue shift between zebrafish and mouse

Because of the high similarity of the early expression pattern of zebrafish *gbx1* with the early *Gbx2* expression in other species, and the relatively late activation of the zebrafish *gbx2* homologue at the MHB, we propose that the functional requirement may be distributed differently in zebrafish as compared to mammals, in that *gbx1*, instead of *gbx2*, may be required early in zebrafish development for the correct specification of the MHB primordium, similar to the early *Gbx2* expression in mice. Another possible example of such an evolutionary switch, or orthologue-shift, between fish and mouse, may be the requirement for early *engrailed* gene function: in fish, *eng2a* and *eng2b* (formerly *eng2* and *eng3*) are the key early genes involved in MHB development. They are the orthologues of En2, which performs a later function in mice than En1 (Scholpp and Brand, 2001; Force et al., 1999). Such paralogue shifts may more generally contribute to the evolution of gene functions in vertebrates.

4. Experimental procedures

4.1. Cloning, mapping and synteny of zebrafish gbx1 and gbx2

A partial *gbx1* cDNA clone was isolated in a large scale in-situ hybridisation screen of random cDNA clones for spatially restricted expression patterns (Thisse et al., 2001); a full length clone was obtained by screening a gastrula stage cDNA library. The *gbx2* clone has been isolated in a screen for homeobox genes from a cosmid library (Amores et al., 1998). Genbank accession numbers: *gbx2*: AF288762, *gbx1*: AF288763.

We mapped the *gbx2* gene on the MOP meiotic mapping cross by single strand conformation polymorphism (Postlethwait et al., 1998) using primers F-GGTCTCTGC TGAAGCACA; R-TGAGCCCTATAGCCAACAGAT. The position of *gbx2* was then intercalated into the HS meiotic mapping panel (Woods et al., 2000) from its position relative to closely linked flanking markers positioned on the MOP and HS panels. We mapped *gbx1* on the LN54 and Goofellow radiation hybrid panels (Hukriede et al., 1999, 2001; Geisler et al., 1999) using the primers F-GCGGTGCGGAGTCAACATCA and R-AACACGGGGAAATCAGACAACAAA, and the resulting position was intercalated into the HS panel using closely linked flanking markers held in common. The loci *ercc3, sarcosin, ssb, chrna1, nop5, ndufs1, ehh, hdlbp, cul1*, and *erp70* were mapped on the HS panel by Woods et al. (2000). Positions of *mcm6* (fb30d05, T51 panel Y. Zhou) and *sdpr* (fb39c08, LN54 panel, I. Dawid) were obtained from ZFIN (http://zfin.org/) and intercalated into the HS panel.

To determine the phylogenetic affinities, we used the blastx algorithm (http://www.ncbi.nlm.nih.gov/BLAST/) to identify sequences similar to zebrafish *gbx* coding domains. The aligned portion of the *Drosophila unplugged* was chosen as the outgroup. This portion of the *Drosophila* gene was then used in a tblastn search, and sequences showing the highest levels of sequence similarity were imported into CLUSTALX (Julie Thompson and Francois Jeanmougin, ftp://ftp-igbmc.u-strasbg.fr/pub/ClustalX). The fully trimmed unambiguous sequence alignments are available on request. Neighbor-joining trees were drawn with NJPlot (http://pbil.univ-lyon1.fr/software/njplot.html). The statistical robustness of each node was estimated by bootstrapping analysis with 1000 runs (Efron and Gong, 1983; Felsenstein, 1985; Swofford et al., 1996). Sequences used are: Fly *Drosophila melanogaster* (Dme) NM_057798 *unpg*; Chicken *Gallus gallus* (Gga) AB050015 *Gbx-1* and AF022151 *Gbx-2*; Mouse *Mus musculus* (Mmu) XM_144233 *Gbx1* and L39770 *Gbx2*; Frog *Xenopus laevis* (Xla) L47990 *XELXGBX2R* and AF395825 *GBX-2b*; Human *Homo sapiens* (Hsa) XM_069853 *GBX1* and AF118452 *GBX2*; Zebrafish *Danio rerio* (Dre) AF288763 *gbx1* and AF288762 *gbx2*; and Carp *Cyprinus carpio* (Cca) X99910 *ovx1*.

4.2. Whole mount in-situ hybridisation and immunostaining

Digoxigenin or Fluorescein labeled RNA probes were prepared from linearised templates using an RNA labeling and detection kit (Roche Biochemicals); hybridisation and detection with anti-Digoxigenin or anti-Fluorescein antibodies coupled to alkaline phosphatase (Boehringer) is described in Reifers et al. (1998). To determine overlap in double ISH with BM purple and FastRed fluorescent substrate (Roche), the BM purple reaction was allowed to proceed until it quenched but did not obliterate the fluorescent FastRed signal. Stained embryos were dissected and thick sections were prepared with sharpened tungsten needles, mounted in glycerol, and photographed on a Zeiss axiophot. Probes and wild-type expression patterns are described in: *krox20*: Oxtoby and Jowett (1993); *otx2*: Mercier et al. (1995); *pax2.1*: Krauss et al. (1991); *EphA4*: Xu et al. (1994), *papc*: Yamamoto et al. (1998).

For antibody staining against EN 4D9 (ntl/T), embryos were blocked 1 h in (PBS 1×, Triton 0.1%, DMSO 1%, Normal Goat Serum 10%). After blocking, the embryos were incubated in the blocking solution containing 1:500 EN 4D9 antibody for overnight at 4 °C. They were then washed in PBS 1×, Triton 0.1%, DMSO 1%, three times for 20 min and incubated with the second antibody (1:200 anti-rubbit IgG peroxydase conjugated antibody, Sigma) for overnight at 4 °C. After the washing, the signals were detected with DAB (Sigma).

4.3. Zebrafish strains and SU5402 treatment

Zebrafish were raised and kept under standard laboratory conditions at about 28 °C (Westerfield, 1994). To obtain mutant embryos, two heterozygous carriers for the respective mutation were crossed to one another. SU5402 inhibitor (Mohammadi et al., 1997; Calbiochem) treatments were done at 8 uM as described (Reifers et al., 2000). Maternal Zygotic *Oep* (M*Zoep*) fish where generated as described in Gristman et al. (1999).

4.4. Transplantation

WT embryos were labeled by injecting a mixture of 7.5% tetramethylrhodamine and biotin conjugated lysine fixable dextran, 10.000 MW (mini-ruby, Molecular Probes D-3312). WT donor cells were transplanted into unlabeled host embryos derived from an incross of heterozyous *ace* carriers. Transplantations were done at shield stage using a beveled borosilicate capillary. Transplanted cells are visualised with the Vectastain ABC system (VectorsLabs) and DAB (Sigma).

Acknowledgements

We thank all members of the Brand lab for support and a great atmosphere; Karla Neugebauer and Arndt Siekmann for critical reading of the manuscript; Florence Schlotter and Michaela Werner for excellent technical help; Bernard Thisse and Christine Thisse, as well as J.A. Campos-Ortega, for generously providing the initial *gbx1* cDNA, and the gastrula stage cDNA library, respectively. This work was supported by grants from the Deutsche Forschungsgemeinschaft, the EU-Biotech program (QLG3-CT-2001-02310), and the Max-Planck-Society to MB, an Institut National de la Santé et de la Recherche Médicale fellowship to MR, and grants P01HD22486 and R01RR10715 from National Institutes of Health to JHP.

References

Acampora, D., Mazan, S., Avantaggiato, V., Barone, P., Tuorto, F., Lallemand, Y., Brulet, P., Simeone, A., 1996. Epilepsy and brain abnormalities in mice lacking *Otx1* gene. Nat. Genet. 14, 218–222.

Alexander, J., Rothenberg, M., Henry, G.L., Stainier, D.Y., 1999. Casanova plays an early and essential role in endoderm formation in zebrafish. Dev. Biol. 215, 343–357.

Amores, A., Force, A., Yan, Y.L., Joly, L., Amemiya, C., Fritz, A., Ho, R.K., Langeland, J., Prince, V., Wang, Y.L., Westerfield, M., Ekker, M., Postlethwait, J.H., 1998. Zebrafish hox clusters and vertebrate genome evolution. Science 282, 1711–1714.

Ang, S.L., Conlon, R.A., Jin, O., Rossant, J., 1994. Positive and negative signals from mesoderm regulate the expression of mouse *Otx2* in ectoderm explants. Development 120, 2979–2989.

Ang, S.L., Jin, O., Rhinn, M., Daigle, N., Stevenson, L., Rossant, J., 1996. A targeted mouse Otx2 mutation leads to severe defects in gastrulation and formation of axial mesoderm and to deletion of rostral brain. Development 122, 243–252.

Beddington, R.S., Robertson, E.J., 1998. Anterior patterning in mouse. Trends Genet. 14, 277–284.

Belting, H.G., Hauptmann, G., Meyer, D., Abdelilah-Seyfried, S., Chitnis, A., Eschbach, C., Söll, I., Thisse, C., Thisse, B., Artinger, K.B., Lunde, K., Driever, W., 2001. *Spiel ohne grenzen/pou2* is required during establishement of the zebrafish midbrain–hindbrain boundary orgainzer. Development 128, 4165–4176.

Bouillet, P., Chazaud, C., Oulad-Abdelghani, M., Dolle, P., Chambon, P., 1995. Sequence and expression pattern of the Stra7 (Gbx-2) homeobox-containing gene induced by retinoic acid in P19 embryonal carcinoma cells. Dev. Dyn. 204, 372–382.

Brand, M., Heisenberg, C.-P., Jiang, Y.-J., Beuchle, D., Lun, K., van Eeden, F.J.M., Furutani-Seiki, M., Granato, M., Haffter, P., Hammerschmidt, M., Kane, D.A., Kelsh, R.N., Mullins, M.C., Odenthal, J., Nüsslein-Volhard, C., 1996. Mutations in zebrafish genes affecting the formation of the boundary between midbrain and hindbrain. Development 123, 179–190.

Broccoli, V., Boncinelli, E., Wurst, W., 1999. The caudal limit of Otx2 expression positions the isthmic organizer. Nature 401, 164–168.

von Bubnoff, A., Schmidt, J.E., Kimelman, D., 1996. The Xenopus laevis homeobox gene Xgbx-2 is an early marker of anteroposterior patterning in the ectoderm. Mech. Dev. 54, 149–160.

Burgess, S., Reim, G., Chen, W., Hopkins, N., Brand, M., 2002. The *zebrafish spiel-ohne-grenzen (spg)* gene encodes the Pou domain protein Pou2 related to mammalian Oct4 and is essential for pre-gastrula morphogenesis. Development 129, 905–916.

Chandrasekhar, A., Moens, C.B., Warren, J.T. Jr., Kimmel, C.B., Kuwada, J.Y., 1997. Development of branchiomotor neurons in zebrafish. Development 124, 2633–2644.

Chapman, G., Rathjen, P.D., 1995. Sequence and evolutionary conservation of the murine Gbx-2 homeobox gene. FEBS Lett. 364, 289–292.

Chapman, G., Remiszewski, J.L., Webb, G.C., Schulz, T.C., Bottema, C.D., Rathjen, P.D., 1997. The mouse homeobox gene, Gbx2: genomic organization and expression in pluripotent cells in vitro and in vivo. Genomics 46, 223–233.

Chiang, C., Young, K.E., Beachy, P.A., 1995. Control of *Drosophila* tracheal branching by the novel homeodomain gene unplugged, a regulatory target for genes of the bithorax complex. Development 121, 3901–3912.

Crossley, P.H., Martin, G.R., 1995. The mouse Fgf8 gene encodes a family of polypeptides and is expressed in regions that direct outgrowth and patterning in the developing embryo. Development 121, 439–451.

Crossley, P.H., Martinez, S., Martin, G.R., 1996. Midbrain development induced by FGF8 in the chick embryo. Nature 380, 66–68.

Cui, X., Doe, C.Q., 1995. The role of the cell cycle and cytokinesis in regulating neuroblast sublineage gene expression in the *Drosophila* CNS. Development 10, 3233–3243.

Efron, B., Gong, G., 1983. A leisurely look at the bootstrap, the jacknife, and crossvalidation. Am. Stat. 37, 36–48.

Erter, C.E., Solnica-Krezel, L., Wright, C.V., 1998. Zebrafish nodal-related 2 encodes an early mesendodermal inducer signaling from the extraembryonic yolk syncytial layer. Dev. Biol. 204, 361–372.

Erter, C.E., Wilm, T.P., Basler, N., Solnica-Krezel, L., 2001. Wnt8 is required in lateral mesendoderm precursors for neural posteriorization in vivo. Development 128, 3571–3583.

Fainsod, A., Greunbaum, Y., 1989. A chicken homeo box gene with developmentally regulated expression. FEBS Lett. 250, 381–385.

Favor, J., Sandulache, R., Neuhäuser-Klaus, A., Pretsch, W., Chatterjee, B., Senft, E., Wurst, W., Blanquet, V., Grimes, P., Spörle, R., Schughart, K., 1996. The mouse Pax21Neu mutation is identical to a human PAX2 mutation in a family with renal-coloboma syndrome and results in developmental defects of the brain, ear, eye and kidney. Proc. Natl Acad. Sci. 93, 13870–13875.

Fekany, K., Yamanaka, Y., Leung, T., Sirotkin, H.I., Topczewski, J., Gates, M.A., Hibi, M., Renucci, A., Stemple, D., Radbill, A., Schier, A.F., Driever, W., Hirano, T., Talbot, W.S., Solnica-Krezel, L., 1999. The zebrafish bozozok locus encodes Dharma, a homeodomain protein essential for induction of gastrula organizer and dorsoanterior embryonic structures. Development 126, 1427–1438.

Felsenstein, J., 1985. Confidence limits on phylogenies: an approach using the bootstrap. Evolution 39, 783–791.

Force, A., Lynch, M., Pickett, F.B., Amores, A., Yan, Y.L., Poslethwait, J., 1999. Preservation of duplicate genes by complementary, degenerative mutations. Genetics 151, 1532–1545.

Frohman, M.A., Dickinson, M.E., Hogan, B.L.M., Martin, G.R., 1993. Mapping of GBX-1 to mouse chromosome 5 and GBX-2 to mouse chromosome 1. Mouse Genome 91, 323–325.

Fürthauer, M., Reifers, F., Brand, M., Thisse, B., Thisse, C., 2001. Sprouty4 acts in vivo as a feedback-induced antagonist of Fgf signaling in zebrafish. Development 128, 2175–2186.

Geisler, R., Rauch, G.J., Baier, H., van Bebber, F., Brobeta, L., Dekens, M.P., et al., 1999. A radiation hybrid map of the zebrafish genome. Nat. Genet. 23, 86–89.

Gerber, H.P., Seipel, K., Georgiev, O., Hofferer, M., Hug, M., Rusconi, S., Schaffner, W., 1994. Transcriptional activation modulated by homopolymeric glutamine and proline stretches. Science 263, 808–811.

Gritsman, K., Zhang, J., Cheng, S., Heckscher, E., Talbot, W.S., Schier, A.F., 1999. The EGF-CFC protein One-Eye-Pinhead is essential for nodal signaling. Cell 97, 121–132.

Hidalgo-Sanchez, M., Simeone, A., Alvarado-Mallart, R., 1999. Fgf8 and Gbx2 induction concomitant with Otx2 repression is correlated with midbrain–hindbrain fate of caudal prosencephalon. Development 126, 3191–3203.

Ho, C.Y., Houart, C., Wilson, S.W., Stainier, D.Y., 1999. A role for the extraembryonic yolk syncytial layer in patterning the zebrafish embryo suggested by properties of the hex gene. Curr. Biol. 9, 1131–1134.

Hukriede, N.A., Joly, L., Tsang, M., Miles, J., Tellis, P., Epstein, J.A., Barbazuk, W.B., Li, F.N., Paw, B., Postlethwait, J.H., Hudson, T.J., Zon, L.I., McPherson, J.D., Chevrette, M., Dawid, I.B., Johnson, S.L., Ekker, M., 1999. Radiation hybrid mapping of the zebrafish genome. Proc. Natl Acad. Sci. USA 96 (17), 9745–9750.

Hukriede, N., Fisher, D., Epstein, J., Joly, L., Tellis, P., Zhou, Y., Barbazuk, B., Cox, K., Fenton-Noriega, L., Hersey, C., Miles, J., Sheng, X., Song, A., Waterman, R., Johnson, S.L., Dawid, I.B., Chevrette, M., Zon, L.I., McPherson, J., Ekker, M., 2001. The LN54 radiation hybrid map of zebrafish expressed sequences. Genome Res. 11 (12), 2127–2132.

Joyner, A.L., Liu, A., Millet, S., 2000. Otx2, Gbx1 and Fgf8 interact to position and maintain a mid-hindbrain organizer. Curr. Opin. Cell Biol. 12, 736–741.

Katahira, T., Sato, T., Sugiyama, S., Okafuji, T., Araki, I., Funahashi, J.L., Nakamura, H., 2000. Interaction between Otx2 and Gbx2 defines the organizing center for the optic tectum. Mech. Dev. 91, 43–52.

Kelly, G.M., Greenstein, P., Erezyilmaz, D.F., Moon, R.T., 1995. Zebrafish wnt8 and wnt8b share a common activity but are involved in distinct developmental pathways. Development 121, 1787–1799.

Kimmel, C.B., Ballard, W.W., Kimmel, S.R., Ullmann, B., Schilling, T.F., 1995. Stages of embryonic development of the zebrafish. Dev. Dyn. 203, 253–310.

King, M.W., Ndiema, M., Neff, A.W., 1998. Anterior structural defects by misexpression of Xgbx-2 in early *Xenopus* embryos are associated with altered expression of adhesion molecules. Dev. Dyn. 212, 563–579.

Koos, D.S., Ho, R.K., 1998. The nieuwkoid gene characterizes and mediates a Nieuwkoop-center-like activity in the zebrafish. Curr. Biol. 8, 1199–1206.

Krauss, S., Johansen, T., Korzh, V., Fjose, A., 1991. Expression of the zebrafish paired box gene pax[zf-b] during early neurogenesis. Development 113, 1193–1206.

Levken, A.C., Thorpe, C.J., Waxman, J.S., Moon, R.T., 2001. Zebrafish *wnt8* encodes two Wnt8 proteins on a bicistronic transcript and is required for mesoderm and neuroectoderm patterning. Dev. Cell 1, 103–114.

Li, J.Y.H., Joyner, L.A., 2001. Otx2 and Gbx2 are required for refinement and not induction of the mid-hindbrain gene expression. Development 128, 4979–4991.

Li, Y., Allende, M.L., Finkelstein, R., Weinberg, E.S., 1994. Expression of two zebrafish orthodenticle-related genes in the embryonic brain. Mech. Dev. 48, 229–244.

Li, J.Y.H., Lao, Z., Joyner, A.L., 2002. Changing requirements for Gbx2 in development of the cerebellum and maintenance of the mid/hindbrain organizer. Neuron 36, 31–43.

Liao, E.C., Paw, B.H., Oates, A.C., Pratt, S.J., Postlethwait, J.H., Zon, L.I., 1998. SCL/Tal-1 transcription factor acts downstream of cloche to specify hematopoietic and vascular progenitors in zebrafish. Genes Dev. 12, 621–626.

Lin, X., Swaroop, A., Vaccarino, F.M., Murtha, M.T., Haas, M., Ji, X., Ruddle, F.H., Leckman, J.F., 1996. Characterization and sequence analysis of the human homeobox-containing gene GBX2. Genomics 31, 335–342.

Liu, A., Losos, K., Joyner, A.L., 1999. FGF8 can activate Gbx2 and transform regions of the rostral mouse brain into a hindbrain fate. Development 126, 4827–4838.

Longhurst, T.J., Joss, J.M., 1999. Homeobox genes in the Australian lungfish, *Neoceratodus forsteri*. J. Exp. Zool. 285, 140–145.

Lun, K., Brand, M., 1998. A series of no isthmus (noi) alleles of the zebrafish pax2.1 gene reveals multiple signaling events in development of the midbrain–hindbrain boundary. Development 125, 3049–3062.

Marin, F., Puelles, L., 1994. Patterning of the embryonic avian midbrain after experimental inversions: a polarizing activity from the isthmus. Dev. Biol. 163, 19–37.

Martinez, S., Alvarado-Mallart, R.M., 1989. Rostral cerebellum originates from the caudal portion of the so-called mesencephalic vesicle: a study using chick/quail chimeras. Eur. J. Neurosci. 1, 549–560.

Martinez, S., Wassef, M., Alvarado-Mallart, R.M., 1991. Induction of a mesencephalic phenotype in the 2-day-old chick prosencephalon is preceded by the early expression of the homeobox gene *en*. Neuron 6, 971–981.

Martinez, S., Crossley, P.H., Cobos, I., Rubenstein, J.L., Martin, G.R., 1999. FGF8 induces formation of an ectopic isthmic organizer and isthmocerebellar development via a repressive effect on Otx2 expression. Development 126, 1189–1200.

Martinez-Barbera, J.P., Signore, M., Boyl, P.P., Puelles, E., Acampora, D., Gogoi, R., Schubert, F., Lumsden, A., Simeone, A., 2001. Regionalisation of anterior neuroectoderm and its competence in responding to forebrain and midbrain inducing activities depend on mutual antagonism between OTX2 and GBX2. Development 128, 4789–4800.

Matsui, T., Hirai, M., Hirano, M., Kurosawa, Y., 1993. The HOX complex neighbored by the EVX gene, as well as two other homeobox-containing genes, the GBX-class and the EN-class, are located on the same chromosomes 2 and 7 in humans. FEBS Lett. 336, 107–110.

McMahon, A.P., Joyner, A.L., Bradley, A., McMahon, J.A., 1992. The midbrain–hindbrain phenotype of Wnt-1 − /Wnt-1 − mice results from stepwise deletion of engrailed-expressing cells by 9.5 days postcoitum. Cell 69, 581–595.

Mercier, P., Simeone, A., Cotelli, F., Boncinelli, E., 1995. Expression pattern of two otx genes suggests a role in specifying anterior body structures in zebrafish. Int. J. Dev. Biol. 39, 559–573.

Meyers, E.N., Lewandoski, M., Martin, G.R., 1998. An Fgf8 mutant allelic series generated by Cre- and Flp-mediated recombination. Nat. Genet. 18, 136–141.

Millen, K.J., Wurst, W., Herrup, K., Joyner, A., 1994. Abnormal embryonic cerebellar development and patterning of postnatal foliation in two mouse Engrailed-2 mutants. Development 120, 695–706.

Millet, S., Bloch-Gallego, E., Simeone, A., Alvarado-Mallart, R.M., 1996. The caudal limit of Otx2 gene expression as a marker of the midbrain/hindbrain boundary: a study using in situ hybridisation and chick/quail homotopic grafts. Development 122, 3785–3797.

Millet, S., Campbell, K., Epstein, D.J., Losos, K., Harris, E., Joyner, A.L., 1999. A role for Gbx2 in repression of Otx2 and positioning the mid/hindbrain organizer. Nature 401, 161–164.

Mohammadi, M., McMahon, G., sun, L., Tang, C., Hirth, P., Yeh, B.K., Hubbard, S.K., Schlessinger, J., 1997. Structures of the tyrosine kinase domain of the fibroblast growth factor receptor in complex with inhibitors. Science 276, 955–960.

Morris, V.B., Brammall, J., Byrne, M., Frommer, M., 1997. Hox-type and non-Hox homeobox gene sequences in genomic DNA of the sea urchin *Holopneustes purpurescens*. Gene 201, 107–110.

Niss, K., Leutz, A., 1998. Expression of the homeobox gene GBX2 during chicken development. Mech. Dev. 76, 151–155.

Oxtoby, E., Jowett, T., 1993. Cloning of the zebrafish krox-20 gene (krx-20) and its expression during hindbrain development. Nucleic Acids Res. 21, 1087–1095.

Pfeffer, P.L., Gerster, T., Lun, K., Brand, M., Busslinger, M., 1998. Characterization of three novel members of the zebrafish *Pax2/5/8* family: dependency of *Pax5* and *Pax8* expression on the *Pax2.1 (noi)* function. Development 125, 3063–3074.

Picker, A., Brennan, C., Reifers, F., Böhli, H., Holder, N., Brand, M., 1999. Requirement for zebrafish *acerebellar*/FGF8 in midbrain polarization, mapping and confinement of the retinotectal projection. Development 126, 2967–2978.

Postlethwait, J.H., Yan, Y.-L., Gates, M.A., Horne, S., Amores, A., Brownlie, A., Donovan, A., Egan, E.S., Force, A., Gong, Z., Goutel, C., Fritz, A., Kelsh, R., Knapik, E., Liao, E., Paw, B., Ransom, D., Singer, A., Thomson, M., Abduljabbar, T.S., Yelick, P., Beier, D., Joly, J.-S., Larhammar, D., Rosa, F., Westerfield, M., Zon, L.I., Johnson, S.L., Talbot, W.S., 1998. Vertebrate genome evolution and the zebrafish gene map. Nat. Genet. 18, 345–349.

Postlethwait, J.H., Woods, I.G., Ngo-Hazelett, P., Yan, Y.L., Kelly, P.D., Chu, F., Huang, H., Hill-Force, A., Talbot, W.S., 2000. Zebrafish comparative genomics and the origins of vertebrate chromosomes. Genome Res. 10, 1890–1902.

Puelles, L., Marín, F., Martinez-de-la-Torre, M., Martínez, S., 1996. The midbrain–hindbrain junction: a model system for brain regionalization through morphogenetic neuroepithelial interactions. In: Lonai, P., (Ed.), Mammalian Development, Harwood, pp. 173–197.

Raible, F., Brand, M., 2001. Tight transcriptional control of the ETS domain factors *Erm* and *Pea3* by FGF signaling during early zebrafish nervous system development. Mech. Dev. 107, 105–117.

Rhinn, M., Brand, M., 2001. The midbrain–hindbrain boundary organizer. Curr. Opin. Neurobiol. 11, 34–42.

Rhinn, M., Lun, K., Werner, M. Simeone, A., Brand, M., 2003. Isolation and expression of the homeobox gene *gbx1* during mouse development. In preparation.

Reifers, F., Böhli, H., Walsh, E.C., Crossley, P.H., Stainier, D.Y.R., Brand, M., 1998. Fgf8 is mutated in zebrafish *acerebellar* mutants and is required for maintenance of midbrain–hindbrain boundary development and somitogenesis. Development 125, 2381–2395.

Reifers, F., Adams, J., Mason, I., Schulte-Merker, S., Brand, M., 2000. Overlapping and distinct functions provided by fgf17, a new zebrafish member of the Fgf8/17/18 subgroup of Fgfs. Mech. Dev. 99, 39–49.

Reim, G., Brand, M., 2002. *Spiel-ohne-grenzen/Pou2 (spg)* mediates regional competence to respond to Fgf8 during zebrafish. Development 129, 917–933.

Rowitch, D.H., McMahon, A.P., 1995. *Pax-2* expression in the murine neural plate precedes and encompasses the expression domains of *Wnt-1* and *En-1*. Mech. Dev. 52, 3–8.

Schier, A.F., Neuhauss, S.C., Harvey, M., Malicki, J., Solnica Krezel, L., Stainier, D.Y., Zwartkruis, F., Abdelilah, S., Stemple, D.L., Rangini, Z., Yang,, H., Driever, W., 1996. Mutations affecting the development of the embryonic zebrafish brain. Development 123, 165–178.

Scholpp, S., Brand, M., 2001. Morpholino-induced knockdown of zebrafish engrailed genes, eng2 and eng3, reveals redundant and unique functions in midbrain–hindbrain boundary development. Genesis 30, 129–133.

Shamim, H., Mason, I., 1998. Expression of Gbx-2 during early development of the chick embryo. Mech. Dev. 76, 157–159.

Shamim, H., Mahmood, R., Logan, C., Doherty, P., Lumsden, A., Mason, I., 1999. Sequential roles for Fgf4, En1 and FGF8 in specification and regionalisation of the midbrain. Development 126, 945–959.

Stroband, H.W., Dekens, M.P.S., te Kronnie, G., Schipper, H., Samallo, J., 1998. The carp homeobox gene Ovx1 shows early expression during gastrulation and subsequently in the vagal lobe, the facial lobe and the ventral telencephalon. Dev. Genes Evol. 208, 56–59.

Su, Y., Meng, A., 2002. The expression of gbx-2 during zebrafish embryogenesis. Mech. Dev. 113, 107–110.

Sutherland, D., Samakovlis, C., Krasnow, M.A., 1996. Branchless encodes a *Drosophila* FGF homolog that controls tracheal cell migration and the pattern of branching. Cell 87, 1091–1101.

Swofford, D.L., Olsen, G.J., Waddell, P.J., Hillis, D.M., 1996. Phylogenetic inference. In: Hillis, D.M., Moritz, C., Mable, B.K. (Eds.), Molecular Systematics, Sinauer, Sunderland, MA, pp. 407–514.

Tallafuss, A., Wilm, T.P., Crozatier, M., Pfeffer, P., Wassef, M., Bally-Cuif, L., 2001. The zebrafish buttonhead-like factor Bts1 is an early regulator of *pax2.1* expression during mid-hindbrain development. Development 128, 4021–4034.

Thisse, B., Pflumio, S., Furthauer, M., Loppin, B., Heyer, V., Degrave, A., Woehl, R., Lux, A., Steffan, T., Charbonnier, X.Q., Thisse, C., 2001 Expression of the zebrafish genome during embryogenesis. Zfin (http://zfin.org), direct data submission.

Thomson, J.A., Itskovitz-Eldor, J., Shapiro, S.S., Waknitz, M.A., Swiergiel, J.J., Marshall, V.S., Jones, J.M., 1998. Embryonic stem cell lines derived from human blastocysts. Science 282, 1145–1147.

Tour, E., Pillemer, G., Gruenbaum, Y., Fainsod, A., 2002. Gbx2 interacts with Otx2 and patterns the anterior–posterior axis during gastrulation in *Xenopus*. Mech. Dev. 112, 141–151.

Urbanek, P., Wang, Z.Q., Fetka, I., Wagner, E.F., Busslinger, M., 1994. Complete block of early B cell differentiation and altered patterning of the posterior midbrain in mice lacking *Pax5/BSAP*. Cell 79, 901–912.

Wassarman, K.M., Lewandoski, M., Campbell, K., Joyner, A.L., Rubenstein, J.L., Martinez, S., Martin, G.R., 1997. Specification of the anterior hindbrain and establishment of a normal mid/hindbrain organizer is dependent on Gbx2 gene function. Development 124, 2923–2934.

Westerfield, M., 1994. The zebrafish book, 2.1 ed, University of Oregon Press, Oregon.

Woo, K., Fraser, S.E., 1995. Order and coherence in the fate map of the zebrafish nervous system. Development 121, 2595–2609.

Woods, I.G., Kelly, P.D., Chu, F., Ngo-Hazelett, P., Yan, Y.-L., Huang, H., Postlethwait, J.H., Talbot, W.S., 2000. A comparative map of the zebrafish genome. Genome Res. 10 (12), 1903–1914.

Wurst, W., Bally-Cuif, L., 2001. Neural plate patterning: upstream and downstream of the isthmic organizer. Nat. Rev. Neurosci. 2, 99–108.

Wurst, W., Auerbach, A.B., Joyner, A.L., 1994. Multiple developmental defects in Engrailed-1 mutant mice: an early mid-hindbrain deletion and patterning defects in forelimbs and sternum. Development 120, 2065–2075.

Xu, Q., Holder, N., Patient, R., Wilson, S.W., 1994. Spatially regulated expression of three receptor tyrosine kinase genes during gastrulation in the zebrafish. Development 120, 287–299.

Yamamoto, A., Amacher, S.L., Kim, S.-H., Geissert, D., Kimmel, C.B., De Robertis, E.M., 1998. Zebrafish paraxial *protocadherin* is a downstream target of *spadetail* involved in morphogenesis of gastrula mesoderm. Development 125, 3389–3397.

Yamanaka, Y., Mizuno, T., Sasai, Y., Kishi, M., Takeda, H., Kim, C.H., Hibi, M., Hirano, T., 1998. A novel homeobox gene, dharma, can induce the organizer in a non-cellautonomous manner. Genes Dev. 12, 2345–2353.